Acta Astronautica 131 (2017) 69–82

Contents lists available at ScienceDirect

Acta Astronautica

journal homepage: www.elsevier.com/locate/aa

Inertial parameter identification using contact force information for an unknown object captured by a space manipulator

Zhongyi Chu[a,*], Ye Ma[a], Yueyang Hou[b], Fengwen Wang[b]

[a] School of Instrument Science and Opto-Electronics, Beihang University, 37 Xueyuan Road, Beijing 100191, China
[b] Shanghai Key Laboratory of Aerospace Intelligent Control Technology, Shanghai Institute of Spaceflight Control Technology, 1555 Zhongchun Road, Shanghai 201109, China

ARTICLE INFO

Keywords:
Space unknown object
Inertial parameter
Contact force
RLS-APSA
Identification

ABSTRACT

This paper presents a novel identification method for the intact inertial parameters of an unknown object in space captured by a manipulator in a space robotic system. With strong dynamic and kinematic coupling existing in the robotic system, the inertial parameter identification of the unknown object is essential for the ideal control strategy based on changes in the attitude and trajectory of the space robot via capturing operations. Conventional studies merely refer to the principle and theory of identification, and an error analysis process of identification is deficient for a practical scenario. To solve this issue, an analysis of the effect of errors on identification is illustrated first, and the accumulation of measurement or estimation errors causing poor identification precision is demonstrated. Meanwhile, a modified identification equation incorporating the contact force, as well as the force/torque of the end-effector, is proposed to weaken the accumulation of errors and improve the identification accuracy. Furthermore, considering a severe disturbance condition caused by various measured noises, the hybrid immune algorithm, Recursive Least Squares and Affine Projection Sign Algorithm (RLS-APSA), is employed to decode the modified identification equation to ensure a stable identification property. Finally, to verify the validity of the proposed identification method, the co-simulation of ADAMS-MATLAB is implemented by multi-degree of freedom models of a space robotic system, and the numerical results show a precise and stable identification performance, which is able to guarantee the execution of aerospace operations and prevent failed control strategies.

1. Introduction

On-orbit operation is an extremely important and highly competitive field in space technology, with frequent aerospace operations being planned for the near future. Unmanned space operation, eliminating danger to astronauts and greatly reducing operating costs, plays an indispensable role in space activities including the capture, docking, repair, and maintenance of space structures on-orbit [1]. Capturing a space unknown object by a manipulator (or space robotic arm) mounted on a free-floating spacecraft causes changes in the attitude and trajectory of the spacecraft, for the reason that there exists strong dynamic and kinematic coupling between the manipulator and the free-floating spacecraft [2]. This poses a severe challenge to the spacecraft control system's ability to satisfy the accuracy requirement for the orbit and attitude of the spacecraft, considering the uncertain properties of the captured object. To enable a precise control strategy and ensure the normal operating condition of the spacecraft, the inertial parameters (mass, centroid, inertial tensor) of the unknown object should be acquired for the sake of developing a control strategy and executing aerospace operations [3].

For identifying the inertial parameters of a space unknown object, the kinematic properties of the unknown object relative to the inertial-coordinate frame should be obtainedpreferentially. Considering the strong coupling and nonlinear characteristics of spatial parameter identification, schemes of identifying the inertial parameters of a subaerial object [4,5] become invalid. In [6], Yoshisada Murotsu proposed two parameter-identification schemes for a space unknown object based on the momentum conservation equation (MC) and equations of motion (EM) in the post-capture phase [1], which were put forward by considering the reason that the system composed of the spacecraft, manipulator and unknown object (space robotic system [1]) is not subject to external force, so it satisfies the conservation of linear or angular momentum and the conservation of internal force or moment. By acquiring the kinematic information of the system using sensors mounted in the system, the kinematics of the captured unknown object can be estimated and resolved. Kazuya Yoshida [7]

* Corresponding author.
E-mail address: chuzystar@gmail.com (Z. Chu).

http://dx.doi.org/10.1016/j.actaastro.2016.11.019
Received 11 March 2016; Accepted 11 November 2016
Available online 17 November 2016
0094-5765/

proposed a scheme of identifying the inertial parameters of a free-flying spacecraft using the MC method by considering the gravity gradient effect. Roberto Lampariello [8] identified the inertial parameters of a free-flying spacecraft and also an unknown object by an accelerometer mounted on the spacecraft, based on the EM method. Ou Ma [9] identified the properties of a spacecraft by changing the inertia distribution of the spacecraft system using the MC method. Thai Chau [10] proposed "adaptive reactionless motion" identification on the basis of the MC method. In the process of the capture and parameter identification, the motions of the manipulator make a minimum disturbance to the spacecraft using an adaptive reactionless control (ARLC) algorithm. Panfeng Huang [11] proposed a takeover control strategy for the unknown object during the post-capture phase by using a space robot, and the unknown property of captured object is coped with the reconfigurable control system. And methods based on vision with spacecraft-mounted cameras capturing the kinematic information of the unknown object [12,13] are also used to identify the centroid and ratios of inertia in the pre-capture phase. A tethered robotic system identifying the inertial parameters of unknown objects in the post-capture phase using the EM method is presented in [14], and the strategy of coordinated control by the orbit and attitude simultaneously for the tethered robotic system is considered in [15]. The principles mentioned above to identify the inertial parameters of a space unknown object can be divided into two categories: one based on solving for the kinematic property (linear or angular velocity) of an object by the conservation of momentum equation (MC) and the other focusing on analysing the dynamic property (accelerator or force) of an object by the equations of Newton-Euler or Lagrange (EM). Both methods have an identical nature in constructing a linear identification equation by which to estimate the intact inertial parameters and only requiring velocity measurements for the inertial parameter identification in the post-capture phase. Compared with the EM method including acceleration measurement, the MC method has superior measured data without being more susceptible to signal noise.

Generally, the unknown inertial parameters are treated as solutions of the linear identification equation [6], and the coefficients of the identification equation determine the validity of the solutions. Based on the components of the coefficient matrix or vector from the identification equation, the solutions, i.e., the inertial parameters of the unknown object, can be dominated by two factors: the kinematic property of the unknown object and the inertial property of the spacecraft and manipulator. Mainly allocated by the linear and angular velocity, the kinematic property of the unknown object can be obtained by conventional schemes including the MC and EM methods mentioned above, and the inertial property containing the mass, centroid and inertial tensor of the spacecraft and manipulator is regarded as prior knowledge. To the best knowledge of the authors, most existing reports [6–16] assume the ideal acquirement of the kinematic and inertial properties without measured or estimated errors, which does not represent the practical condition of parameter identification. In fact, with inevitable disturbances from the complicated outer space environment and uncertainties in the measurements of the sensors, the errors caused by the kinematic measurement are directly introduced to the identification equation and induce poor precision in the inertial parameters to be identified. In addition, the inertial parameters of a spacecraft are not always constant with frequent aerospace operations, e.g., fuelconsumption, and a measurement or estimation process for spacecraft is needed in the aerospace condition [7–9], which can also be accompanied by estimation error. Therefore, two errors need to be considered in the identification equation of an unknown object, including errors from the measured kinematic information of the unknown object and errors from the estimated inertial parameters of the spacecraft and manipulator. In [8], an error estimation for identifying the inertial parameters of a spacecraft is illustrated by the error-bound estimation method. However, there has been no specialized study on the influence of measurement or estimation errors on the identification precision of a captured unknown object. An analysis of the effect of errors to the identification process is essential, and a scheme is required for practical implementation.

Based on the further study in this paper, in the accumulative calculation process from the spacecraft to the end of the manipulator (end-effector), even a faint disturbance to the nominal kinematic values of a spacecraft can have an immense influence on the ultimate identification results of the unknown object. In the construction of the coefficient matrix or the vector of the identification equation by the measured information, the accumulated kinematic measurement errors and inertial estimation errors mainly account for the poor performance of parameter identification. Therefore, to weaken the accumulation of the kinematic measurement errors of the unknown object and the inertial estimation errors of the spacecraft, a straightaway mode of measurement without too much accumulation is accommodated to improve the identification accuracy. In this paper, based on the momentum theorem, information on a contact force acting on the surface of a space unknown object attached to the force/torque information of the end-effector is employed to modify the conventional identification equation, for the reason that the contact force information directly reflects the state of stress of the captured unknown object, without theoreticaldeduction by the accumulated kinematic information from the spacecraft and manipulator. The force/torque information of the end-effector has the "closest" access to the rotational motion information of the unknown object, enabling the identification of the inertial tensor of the unknown object without too much accumulated calculation. According to the momentum theorem, the increment of the linear/angular momentum of an unknown object from the MC method can be replaced by the linear/angular impulse, i.e., the integration by the resultant force or torque of the unknown object, which can be obtained by the measured information of the contact force as well as the force/torque of the end-effector. The use of the integration of the force or torque to replace the linear/angular momentum from the MC method effectively weakens the components of the calculated momentum of the unknown object in the conventional identification equation, avoiding excessive measured and estimated information from the spacecraft and thereby reducing error sources in the identification process. It is valuable to mention that the detection and application of the contact force has the feature of flexibility [17], and the detecting system incorporating the measured contact force accompanied by the force/torque of the end-effector has been adopted by many end-effectors in practice [18,19] and has been proven to be a practical and feasible measuring mode for use in aerospace operation.

In this paper, a novel identification scheme based on the contact force information of the unknown object along with the force/torque information of the end-effector is proposed, in which the calculated momentum information from the MC method is replaced by the integration of the contact force together with the force/torque of the end-effector to improve the identification precision by weakening the accumulated kinematic measurement errors of the unknown object as well as the inertial estimation errors of the spacecraft and manipulator. The innovation of the work includes the following three points: the first is a systematic analysis of the effect of the kinematic measurement errors on the identification precision of the space unknown object from the conventional method; the second is a modification of the identification equation by incorporating the contact force and force/torque information of the end-effector to improve the precision; and the third is the use of the hybrid immune algorithm of RLS-APSA to decode the modified identification equation and ensure a stable identification property.

Section 2 first describes the basic theory of identification, including the kinematics of the robotic system with an n-degree-of-freedom (n-DOF) manipulator and the conventional identification equation. Followed by a description of the process of error estimation, a systematic analysis of the effect of kinematic measurement errors on the identification precision of the conventional method is illustrated. Then, a modified identification equation incorporating the contact force and force/torque of the end-effector is presented in Section 3 to improve the precision. The hybrid immune algorithm of RLS-APSA is proposed to decode the modified identification equation and ensure the stability of identification, considering a severe disturbance condition with various measured noises. In Section 4, to verify the validity of the proposed identification scheme, the dynamic model of the space robotic system (with the 3-DOF and 7-DOF manipulator) is established by ADAMS, and the identification process is implemented by a constructed ADAMS-MATLAB co-simulation platform. The numerical simulation results prove the improved stability and accuracy achieved with the proposed scheme. Section 5 presents the conclusions and suggests future research work.

2. Analysis of the kinematic measurement errors

2.1. Basic theory of identification

A rigid robotic system composed of a spacecraft, manipulator (n-degree-of-freedom) and space unknown object in the post-capture phase is derived in this section, as shown in Fig. 1. The condition of conservation of momentum can be fulfilled with a space robotic system [6,10], considering a spacecraft in a free-floating state and neglecting the effect of microgravity in a short time. From Fig. 1, Σ_I, Σ_B, Σ_i, Σ_U are the inertial coordinate frame and the body coordinate frames of the spacecraft, link i and unknown object, respectively; $\boldsymbol{p_B}(\boldsymbol{p}_0)$, $\boldsymbol{p_i}$, $\boldsymbol{p_U}(\boldsymbol{p}_{n+1})$ are the positions vector of the reference point of the body frame onthespacecraft, joint i and unknown object, respectively, expressed in Σ_I; $\boldsymbol{r_B}(\boldsymbol{r}_0)$, $\boldsymbol{r_i}$, $\boldsymbol{r_U}$ are the position vectors of the centroids ofthe spacecraft, link i and unknown object, respectively, expressed in Σ_I; $\boldsymbol{\omega_B}(\boldsymbol{\omega}_0)$, $\boldsymbol{\omega_i}$, $\boldsymbol{\omega_U}$ are the angular velocity vectors of the spacecraft, link i and unknown object, respectively, expressed in Σ_I; and $\boldsymbol{\theta}_i$ is the angle vector formed by the output of the encoder installed in joint i, expressed in Σ_I. There exists a geometric relationship of $\boldsymbol{a_B}(\boldsymbol{a}_0)$, $\boldsymbol{b_B}(\boldsymbol{b}_0)$, $\boldsymbol{a_i}$, $\boldsymbol{b_i}$, $\boldsymbol{a_U}$ from Eqs. (1)–(3)[6,16].

$$\boldsymbol{a_i} = \boldsymbol{r_i} - \boldsymbol{p_i} \quad (i = 0,\ 1,\ \ldots n) \tag{1}$$

$$\boldsymbol{b_i} = \boldsymbol{p}_{i+1} - \boldsymbol{r_i} \quad (i = 0,\ 1,\ \ldots n) \tag{2}$$

$$\boldsymbol{a_U} = \boldsymbol{r_U} - \boldsymbol{p_U} \tag{3}$$

$$\boldsymbol{\omega_i} = \boldsymbol{\omega}_{i-1} + \dot{\boldsymbol{\theta}}_i \ (i = 1,\ 2,\ldots,n) \tag{4}$$

$$\dot{\boldsymbol{r}}_i = \dot{\boldsymbol{p}}_i + \boldsymbol{\omega_i} \times \boldsymbol{a_i} \quad (i = 0,\ 1,\ldots,n) \tag{5}$$

$$\dot{\boldsymbol{p}}_i = \dot{\boldsymbol{r}}_{i-1} + \boldsymbol{\omega}_{i-1} \times \boldsymbol{b}_{i-1} \quad (i = 1,\ 2,\ldots,n) \tag{6}$$

$$\boldsymbol{\omega_U} = \boldsymbol{\omega}_n \tag{7}$$

$$\dot{\boldsymbol{p}}_U = \dot{\boldsymbol{r}}_n + \boldsymbol{\omega}_n \times \boldsymbol{b}_n \tag{8}$$

$$\dot{\boldsymbol{r}}_U = \dot{\boldsymbol{p}}_U + \boldsymbol{\omega_U} \times \boldsymbol{a_U} \tag{9}$$

Considering the kinematics of the space robotic system in the post-capture phase, Eqs. (4)–(9) are expressed briefly in the inertial frame. Here, it is assumed that the system consists of rigid bodies only with no external forces or torques existing in the system. The employment of the reaction wheels and other momentum-exchange devices is not considered in this study. And the unknown object is grasped firmly by the manipulator in the post-capture phase, with the relative position and orientation of the unknown object to the manipulator not changing. From [6,16], the linear and angular momentums of the whole space robotic system are supposed to be zero. Therefore, the Eqs. (10)–(12) can be illustrated as follows.

$$\boldsymbol{P} = m_B\dot{\boldsymbol{r}}_B + \sum_{i=1}^{n} m_i\dot{\boldsymbol{r}}_i + m_U\dot{\boldsymbol{r}}_U \tag{10}$$

$$\boldsymbol{L} = \boldsymbol{I_B}\boldsymbol{\omega_B} + \sum_{i=1}^{n}\boldsymbol{I_i}\boldsymbol{\omega_i} + \boldsymbol{I_U}\boldsymbol{\omega_U} + \boldsymbol{r_B} \times m_B\dot{\boldsymbol{r}}_B + \sum_{i=1}^{n}\boldsymbol{r_i} \times m_i\dot{\boldsymbol{r}}_i + \boldsymbol{r_U} \times m_U\dot{\boldsymbol{r}}_U \tag{11}$$

$$\begin{Bmatrix} -{}^{U}\dot{\boldsymbol{p}}_U \\ {}^{U}\boldsymbol{L_K} \end{Bmatrix} = \begin{Bmatrix} {}^{U}\boldsymbol{P_K} & [{}^{U}\boldsymbol{\omega}_U^{\times}] & 0 \\ 0 & [{}^{U}\boldsymbol{P}_K^{\times}] & [\#^{U}\boldsymbol{\omega}_U] \end{Bmatrix} \begin{Bmatrix} \frac{1}{m_U} \\ {}^{U}\boldsymbol{a_U} \\ {}^{U}\boldsymbol{I}_U^{\#} \end{Bmatrix} \tag{12}$$

From Eqs. (10) and (11), $\boldsymbol{P}$ and $\boldsymbol{L}$ denote the linear momentum and angular momentum of the whole space robotic system, respectively, expressed in the inertial frame; $m_B(m_0)$, m_i, and m_U are the masses of the spacecraft, link i and unknown object, respectively. $\boldsymbol{I}_B(\boldsymbol{I}_0)$, $\boldsymbol{I_i}$, and $\boldsymbol{I}_U$ are the inertial tensors relative to the individual centroids of the spacecraft, link i and unknown object, respectively. From the linear identification Eq. (12), m_U, $\boldsymbol{a_U}$ and $\boldsymbol{I}_U$ are the inertial parameters of the unknown object to be identified, and ${}^{U}\boldsymbol{P_K}$, ${}^{U}\boldsymbol{L_K}$, ${}^{U}\dot{\boldsymbol{p}}_U$, ${}^{U}\boldsymbol{\omega_U}$, ${}^{U}\boldsymbol{a_U}$, and ${}^{U}\boldsymbol{I_U}$ are matrices (vectors) of $\boldsymbol{P_K}$, $\boldsymbol{L_K}$, $\dot{\boldsymbol{p}}_U$, $\boldsymbol{\omega_U}$, $\boldsymbol{a_U}$, and $\boldsymbol{I}_U$ in the inertial frame, expressed in Σ_U. From [6,16], $\boldsymbol{P_K}$, $\boldsymbol{L_K}$, $\boldsymbol{\omega_U}^{\times}$, $\#\boldsymbol{\omega_U}$, and $\boldsymbol{I}_U^{\#}$ can be described by Eqs. (13)–(17) as follows.

$$\boldsymbol{P_K} = m_B\dot{\boldsymbol{r}}_B + \sum_{i=1}^{n} m_i\dot{\boldsymbol{r}}_i \tag{13}$$

$$\boldsymbol{L_K} = -\boldsymbol{I_B}\boldsymbol{\omega_B} - \sum_{i=1}^{n}\boldsymbol{I_i}\boldsymbol{\omega_i} - m_B\dot{\boldsymbol{r}}_B \times (\boldsymbol{b_B} + \sum_{i=1}^{n}(\boldsymbol{a_i} + \boldsymbol{b_i})) - \sum_{i=1}^{n} m_i\dot{\boldsymbol{r}}_i \times (\boldsymbol{L_i})$$
$$\boldsymbol{L_i} = \boldsymbol{b_i} + \sum_{j=i+1}^{n}(\boldsymbol{a_j} + \boldsymbol{b_j}) \tag{14}$$

$$\boldsymbol{\omega}_U^{\times} = \begin{bmatrix} 0 & -\omega_{Uz} & \omega_{Uy} \\ \omega_{Uz} & 0 & -\omega_{Ux} \\ -\omega_{Uy} & \omega_{Ux} & 0 \end{bmatrix} \tag{15}$$

$$\#\boldsymbol{\omega_U} = \begin{bmatrix} \omega_{Ux} & \omega_{Uy} & \omega_{Uz} & 0 & 0 & 0 \\ 0 & \omega_{Ux} & 0 & \omega_{Uy} & \omega_{Uz} & 0 \\ 0 & 0 & \omega_{Ux} & 0 & \omega_{Uy} & \omega_{Uz} \end{bmatrix} \tag{16}$$

$$\boldsymbol{I}_U^{\#} = [\ I_{Uxx}\ ,\quad I_{Uxy},\quad I_{Uxz},\quad I_{Uyy},\quad I_{Uyz},\quad I_{Uzz}\ ]^T \tag{17}$$

Eq. (12) can be decomposed into the form of Eq. (18).

$$\begin{aligned} -\dot{p}_{Ux} &= P_{Kx}\cdot\frac{1}{m_U} - \omega_{Uz}\cdot a_{Uy} + \omega_{Uy}\cdot a_{Uz} \\ -\dot{p}_{Uy} &= P_{Ky}\cdot\frac{1}{m_U} + \omega_{Uz}\cdot a_{Ux} - \omega_{Ux}\cdot a_{Uz} \\ -\dot{p}_{Uz} &= P_{Kz}\cdot\frac{1}{m_U} - \omega_{Uy}\cdot a_{Ux} + \omega_{Ux}\cdot a_{Uy} \end{aligned} \tag{18-a}$$

$$\begin{aligned} L_{Kx} &= -P_{Kz}\cdot a_{Uy} + P_{Ky}\cdot a_{Uz} + \omega_{Ux}\cdot I_{Uxx} + \omega_{Uy}\cdot I_{Uxy} + \omega_{Uz}\cdot I_{Uxz} \\ L_{Ky} &= P_{Kz}\cdot a_{Ux} - P_{Kx}\cdot a_{Uz} + \omega_{Ux}\cdot I_{Uxy} + \omega_{Uy}\cdot I_{Uyy} + \omega_{Uz}\cdot I_{Uyz} \\ L_{Kz} &= -P_{Ky}\cdot a_{Ux} + P_{Kx}\cdot a_{Uy} + \omega_{Ux}\cdot I_{Uxz} + \omega_{Uy}\cdot I_{Uyz} + \omega_{Uz}\cdot I_{Uzz} \end{aligned} \tag{18-b}$$

From Eq. (18), two crucial conclusions can be illustrated.

First, to ensure that the coefficient matrix of the linear identification Eq. (12) is in a non-singular state, there must exist kinematic information on all the translational and rotational motions from the three orthogonal axes in the inertial frame to maintain the integrity of the identification for all inertial parameters. On account of that the

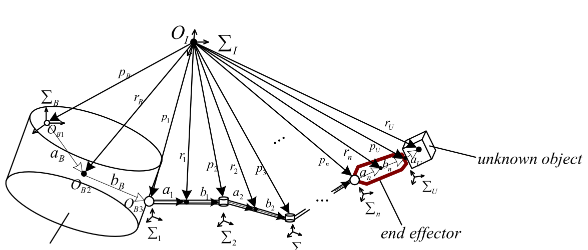

Fig. 1. Spacecraft-manipulator-unknown object system (Space robotic system).

motions of the three orthogonal axes in the inertial frame can be decomposed into the motions of three axes from an arbitrary body frame in the space robotic system, also incorporating Σ_U, the necessary condition of intact identification can be stated using existing translation and rotation motions in all three orthogonal directions from the body frame of the unknown object, which can be ensured by actuating joints of various directions in the post-capture phase [6] or by the collision motivation [10] in the capture-collision phase for the identification of the unknown object.

Second, linear Eq. (12) contains ten inertial parameters (m_U, a_{Ux} , a_{Uy}, a_{Uz}, $\boldsymbol{I}^{\#}{}_U$) to be identified, with strong coupling features of unknown parameters. The ten inertial parameters can be ideally obtained by the perfect coefficient matrix (or vector) of linear Eq. (12), which determines the accuracy of the identified parameters. However, as they are inevitably impacted by measurement or estimation errors, inaccurate coefficients cause poor accuracy of the coupling of the inertial parameters by the coupling Eq. (12). To address the strong coupling of linear Eq. (12), a practical decoupling procedure is essential, andthe linear identification Eq. (12) can thus be decomposed into Eqs. (19) and (20). Therefore, a two-step procedure of identification can be implemented, as shown in Fig. 2, to improve the accuracy of the inertial parameter identification.

$$-\dot{\boldsymbol{p}}_U = \boldsymbol{P}_K\cdot\frac{1}{m_U} + [\boldsymbol{\omega}_U{}^{\times}]\cdot \boldsymbol{a}_U \tag{19}$$

$$\boldsymbol{L}_K - [\boldsymbol{P}_K{}^{\times}]\cdot\boldsymbol{a}_U = [\ \#\boldsymbol{\omega}_U]\cdot[\boldsymbol{I}_U{}^{\#}] \tag{20}$$

From Fig. 2, the mass and centroid of an unknown object can be first obtained by Eq. (19) based on the acknowledged $\boldsymbol{P}_K$, $\boldsymbol{\omega}_U$, and $\dot{\boldsymbol{p}}_U$, and the identified values $\boldsymbol{a}_U$ can be transferred into Eq. (20) as priori knowledge, together with the acknowledged $\boldsymbol{L}_K$ and $\boldsymbol{\omega}_U$ to acquire the inertial tensor of the unknown object. Compared with Eq. (12), which contains ten unknown parameters, the expression of Eq. (19) has fewer coupling features, with only four unknown parameters to identify. The expression of Eq. (20) decreases the coupling of equations by containing six unknown parameters, which is determined and improved by the superior identification result of $\boldsymbol{a}_U$ by the lower coupling equation (19).

2.2. Effect of kinematic measurement errors on the identification precision

From Eqs. (19) and (20), a two-step identification can be performed by the coefficient matrixes$\boldsymbol{\omega}_U{}^{\times}$, $\#\boldsymbol{\omega}_U$ and coefficient vectors $\boldsymbol{P}_K$, $\dot{\boldsymbol{p}}_U$, $\boldsymbol{L}_K - [\boldsymbol{P}_K{}^{\times}]\cdot\boldsymbol{a}_U$. From Eqs. (4)–(9), $\boldsymbol{\omega}_U$,$\dot{\boldsymbol{p}}_U$can be acquired by kinematic deduction from the space robotic system via information$\boldsymbol{\omega}_B$, $\dot{\boldsymbol{p}}_B$, $\dot{\boldsymbol{\theta}}_i$, which can be measured by a rate gyroscope and accelerometer installed on the spacecraft and encoders mounted in all joints of tge manipulator in practice. From Eqs. (13) and (14), $\boldsymbol{P}_K$, $\boldsymbol{L}_K$ depend on inertial parameters and kinematic parameters of the spacecraft and manipulator in the robotic system, of which the inertial parameters can be estimated in aerospace and the kinematic parameters can be calculated from Eqs. (4)–(9) via $\boldsymbol{\omega}_B$, $\dot{\boldsymbol{p}}_B$, $\dot{\boldsymbol{\theta}}_i$. Therefore, the kinematic measured information of $\boldsymbol{\omega}_B$, $\dot{\boldsymbol{p}}_B$, $\dot{\boldsymbol{\theta}}_i$ and the inertial information of the spacecraft and manipulator provides all the data needed to construct the coefficients of the linear Eqs. (19–20), and the measurement errors

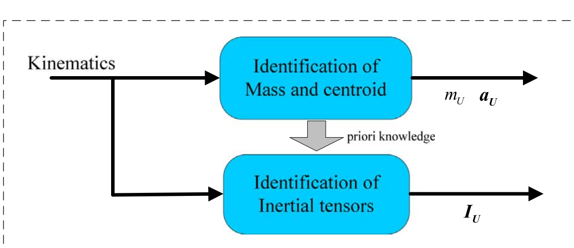

Fig. 2. Two-step identification.

of $\boldsymbol{\omega}_B$, $\dot{\boldsymbol{p}}_B$, $\dot{\boldsymbol{\theta}}_i$ and the estimation errors of the inertial parameters from the spacecraft and manipulators dominate the accuracy of the identified parameters of m_U,$\boldsymbol{a}_U$, $\boldsymbol{I}_U$.

To realize the individual effects of the identified inertial parameters by the kinematic measurement errors from the measured data $\boldsymbol{\omega}_B$,$\dot{\boldsymbol{p}}_B$,$\dot{\boldsymbol{\theta}}_i$, the inertial estimation errors will be ignored in this section, i.e., the inertial parameters of the spacecraft and manipulator are assumed as prior knowledge owning ideal properties without estimation errors in the process of identification.

From Eqs. (19) and (20), with the presence of measurement errors in the process of identification, Eqs. (19) and (20) become Eqs. (21) and (22), respectively,

$$-\tilde{\dot{\boldsymbol{p}}}_U = \tilde{\boldsymbol{P}}_K\cdot\frac{1}{m_U} + [\tilde{\boldsymbol{\omega}}_U{}^{\times}]\cdot \boldsymbol{a}_U \tag{21}$$

$$\tilde{\boldsymbol{L}}_K - [\tilde{\boldsymbol{P}}_K{}^{\times}]\cdot\boldsymbol{a}_U = [\ \#\tilde{\boldsymbol{\omega}}_U]\cdot[\boldsymbol{I}_U{}^{\#}] \tag{22}$$

where

$$\tilde{\dot{\boldsymbol{p}}}_U = \dot{\boldsymbol{p}}_U + \Delta\,\dot{\boldsymbol{p}}_U \tag{23}$$

$$\tilde{\boldsymbol{P}}_K = \boldsymbol{P}_K + \Delta\,\boldsymbol{P}_K,\qquad \tilde{\boldsymbol{P}}_K{}^{\times} = (\boldsymbol{P}_K + \Delta\,\boldsymbol{P}_K)^{\times} = \boldsymbol{P}_K{}^{\times} + (\Delta\,\boldsymbol{P}_K)^{\times} \tag{24}$$

$$\tilde{\boldsymbol{\omega}}_U{}^{\times} = (\boldsymbol{\omega}_U + \Delta\boldsymbol{\omega}_U)^{\times} = \boldsymbol{\omega}_U{}^{\times} + (\Delta\boldsymbol{\omega}_U)^{\times},\qquad \#\tilde{\boldsymbol{\omega}}_U = \#(\boldsymbol{\omega}_U + \Delta\boldsymbol{\omega}_U) = \#\boldsymbol{\omega}_U + \#(\Delta\boldsymbol{\omega}_U) \tag{25}$$

$$\tilde{\boldsymbol{L}}_K = \boldsymbol{L}_K + \Delta\boldsymbol{L}_K \tag{26}$$

The coefficient matrixes $\Delta\boldsymbol{\omega}_U{}^{\times}$, $\Delta\#\boldsymbol{\omega}_U$ and coefficient vectors $\Delta\boldsymbol{P}_K$, $\Delta\boldsymbol{L}_K$, $\Delta\dot{\boldsymbol{p}}_U$ are errors of $\boldsymbol{\omega}_U{}^{\times}$, $\#\boldsymbol{\omega}_U$, $\boldsymbol{P}_K$, $\boldsymbol{L}_K$ and $\dot{\boldsymbol{p}}_U$, which are caused by the kinematic measurement errors of $\boldsymbol{\omega}_B$,$\dot{\boldsymbol{p}}_B$,$\dot{\boldsymbol{\theta}}_i$, namely,$\Delta\boldsymbol{\omega}_B$,$\Delta\dot{\boldsymbol{p}}_B$,$\Delta\dot{\boldsymbol{\theta}}_i$ respectively. Therefore, Eq. (4)–(8) can be rewritten by Eqs. (27)-(35) using the method of induction and also considering thegeometric relationship of Eq. (1)–(3).

$$\tilde{\dot{\boldsymbol{p}}}_B = \dot{\boldsymbol{p}}_B + \Delta\dot{\boldsymbol{p}}_B \tag{27}$$

$$\tilde{\boldsymbol{\omega}}_B = \boldsymbol{\omega}_B + \Delta\boldsymbol{\omega}_B \tag{28}$$

$$\tilde{\dot{\boldsymbol{\theta}}}_i = \dot{\boldsymbol{\theta}}_i + \Delta\dot{\boldsymbol{\theta}}_i \tag{29}$$

$$\begin{aligned}\tilde{\dot{\boldsymbol{r}}}_B &= \tilde{\dot{\boldsymbol{p}}}_B + \tilde{\boldsymbol{\omega}}_B\times\boldsymbol{a}_B = (\dot{\boldsymbol{p}}_B + \Delta\dot{\boldsymbol{p}}_B) + (\boldsymbol{\omega}_B + \Delta\boldsymbol{\omega}_B)\times\boldsymbol{a}_B\\ &= (\dot{\boldsymbol{p}}_B + \boldsymbol{\omega}_B\times\boldsymbol{a}_B) + \Delta\dot{\boldsymbol{p}}_B + \Delta\boldsymbol{\omega}_B\times\boldsymbol{a}_B = \dot{\boldsymbol{r}}_B + \Delta\dot{\boldsymbol{p}}_B + \Delta\boldsymbol{\omega}_B\times\boldsymbol{a}_B\end{aligned} \tag{30}$$

$$\begin{aligned}\tilde{\boldsymbol{\omega}}_i &= \tilde{\boldsymbol{\omega}}_{i-1} + \tilde{\dot{\boldsymbol{\theta}}}_i = \tilde{\boldsymbol{\omega}}_B + \sum_{j=1}^{i}\tilde{\dot{\boldsymbol{\theta}}}_j = (\boldsymbol{\omega}_B + \Delta\boldsymbol{\omega}_B) + \sum_{j=1}^{i}(\dot{\boldsymbol{\theta}}_j + \Delta\dot{\boldsymbol{\theta}}_j)\\ &= (\boldsymbol{\omega}_B + \sum_{j=1}^{i}\dot{\boldsymbol{\theta}}_j) + (\Delta\boldsymbol{\omega}_B + \sum_{j=1}^{i}\Delta\dot{\boldsymbol{\theta}}_j) = \boldsymbol{\omega}_i + \Delta\boldsymbol{\omega}_B\\ &\quad + \sum_{j=1}^{i}\Delta\dot{\boldsymbol{\theta}}_j\ (i = 1, 2, \ldots, n)\end{aligned} \tag{31}$$

$$\begin{aligned}\tilde{\dot{\boldsymbol{p}}}_i &= \tilde{\dot{\boldsymbol{r}}}_{i-1} + \tilde{\boldsymbol{\omega}}_{i-1}\times\tilde{\boldsymbol{b}}_{i-1} = \dot{\boldsymbol{r}}_{i-1} + \Delta\dot{\boldsymbol{r}}_{i-1} + (\boldsymbol{\omega}_{i-1} + \Delta\boldsymbol{\omega}_{i-1})\times\boldsymbol{b}_{i-1}\\ &= (\dot{\boldsymbol{r}}_{i-1} + \boldsymbol{\omega}_{i-1}\times\boldsymbol{b}_{i-1}) + (\Delta\dot{\boldsymbol{r}}_{i-1} + \Delta\boldsymbol{\omega}_{i-1}\times\boldsymbol{b}_{i-1})\\ &= \dot{\boldsymbol{p}}_i + \Delta\dot{\boldsymbol{p}}_B + \Delta\boldsymbol{\omega}_B\times\left[\boldsymbol{a}_B + \boldsymbol{b}_B + \sum_{j=1}^{i-1}(\boldsymbol{a}_j + \boldsymbol{b}_j)\right]\\ &\quad + \sum_{j=1}^{i-1}\left[\Delta\dot{\boldsymbol{\theta}}_j\times\sum_{k=j}^{i-1}(\boldsymbol{a}_k + \boldsymbol{b}_k)\right](i = 1, 2, \ldots, n)\end{aligned} \tag{32}$$

$$\begin{aligned}\tilde{\dot{\boldsymbol{r}}}_i &= \tilde{\dot{\boldsymbol{p}}}_i + \tilde{\boldsymbol{\omega}}_i\times\boldsymbol{a}_i = \dot{\boldsymbol{p}}_i + \Delta\dot{\boldsymbol{p}}_i + (\boldsymbol{\omega}_i + \Delta\boldsymbol{\omega}_i)\times\boldsymbol{a}_i\\ &= \dot{\boldsymbol{p}}_i + \boldsymbol{\omega}_i\times\boldsymbol{a}_i + \Delta\dot{\boldsymbol{p}}_i + \Delta\boldsymbol{\omega}_i\times\boldsymbol{a}_i =\\ &= \dot{\boldsymbol{r}}_i + \Delta\dot{\boldsymbol{p}}_B + \Delta\boldsymbol{\omega}_B\times\left[\boldsymbol{a}_B + \boldsymbol{b}_B + \textstyle\sum_{j=1}^{i-1}(\boldsymbol{a}_j + \boldsymbol{b}_j) + \boldsymbol{a}_i\right]\\ &\quad + \textstyle\sum_{j=1}^{i}\Delta\dot{\boldsymbol{\theta}}_j\times\left[\boldsymbol{a}_j + \textstyle\sum_{k=j}^{i-1}(\boldsymbol{b}_k + \boldsymbol{a}_{k+1})\right](i = 1, 2, \ldots, n)\end{aligned} \tag{33}$$

$$\widetilde{\omega}_U=\widetilde{\omega}_n=\omega_n+\Delta\omega_B+\sum_{i=1}^{n}\Delta\dot{\theta}_i=\omega_U+\Delta\omega_B+\sum_{i=1}^{n}\Delta\dot{\theta}_i \tag{34}$$

$$\begin{aligned}\widetilde{\dot{p}}_U&=\widetilde{\dot{r}}_n+\widetilde{\omega}_n\times\boldsymbol{b}_n=\dot{\boldsymbol{r}}_n+\omega_n\times\boldsymbol{b}_n+\Delta\dot{\boldsymbol{r}}_n+\Delta\omega_n\times\boldsymbol{b}_n\\&=\dot{\boldsymbol{p}}_U+\Delta\dot{\boldsymbol{p}}_B+\Delta\omega_B\times\left[\boldsymbol{a}_B+\boldsymbol{b}_B+\textstyle\sum_{j=1}^{n}(\boldsymbol{a}_j+\boldsymbol{b}_j)\right]\\&\quad+\textstyle\sum_{j=1}^{n}\left[\Delta\dot{\theta}_j\times\sum_{k=j}^{n}(\boldsymbol{a}_k+\boldsymbol{b}_k)\right]\end{aligned} \tag{35}$$

From Eqs. (13) and (14), one can obtain $\widetilde{\boldsymbol{P}}_K$, $\widetilde{\boldsymbol{L}}_K$ from Eq. (36) and (37) as follows.

$$\widetilde{\boldsymbol{P}}_K=m_B\widetilde{\dot{\boldsymbol{r}}}_B+\sum_{i=1}^{n}m_i\widetilde{\dot{\boldsymbol{r}}}_i \tag{36}$$

$$\widetilde{\boldsymbol{L}}_K=-\boldsymbol{I}_B\widetilde{\omega}_B-\sum_{i=1}^{n}\boldsymbol{I}_i\widetilde{\omega}_i-m_B\widetilde{\dot{\boldsymbol{r}}}_B\times(\boldsymbol{b}_B+\sum_{i=1}^{n}(\boldsymbol{a}_i+\boldsymbol{b}_i))-\sum_{i=1}^{n}m_i\widetilde{\dot{\boldsymbol{r}}}_i\times(\boldsymbol{L}_i)$$
$$\boldsymbol{L}_i=\boldsymbol{b}_i+\sum_{j=i+1}^{n}(\boldsymbol{a}_j+\boldsymbol{b}_j) \tag{37}$$

Upon substituting Eqs. (27)–(35) into Eq. (36) and (37), one can obtain Eqs. (38) and (39) as follows.

$$\begin{aligned}\widetilde{\boldsymbol{P}}_K&=m_B\dot{\boldsymbol{r}}_B+\sum_{i=1}^{n}m_i\dot{\boldsymbol{r}}_i+(m_B+\textstyle\sum_{i=1}^{n}m_i)\Delta\dot{\boldsymbol{p}}_B\\&\quad+\Delta\omega_B\times\left\{m_B\boldsymbol{a}_B+\textstyle\sum_{i=1}^{n}m_i\left[\boldsymbol{a}_B+\boldsymbol{b}_B+\boldsymbol{a}_i+\sum_{j=1}^{i-1}(\boldsymbol{a}_j+\boldsymbol{b}_j)\right]\right\}\\&\quad+\textstyle\sum_{i=1}^{n}\Delta\dot{\theta}_i\times\left[\sum_{j=i}^{n}m_j(\boldsymbol{a}_j+\sum_{k=i}^{j-1}(\boldsymbol{a}_k+\boldsymbol{b}_k))\right]\\&=\boldsymbol{P}_K+(m_B+\textstyle\sum_{i=1}^{n}m_i)\Delta\dot{\boldsymbol{p}}_B+\Delta\omega_B\times\\&\quad\left\{m_B\boldsymbol{a}_B+\textstyle\sum_{i=1}^{n}m_i\left[\boldsymbol{a}_B+\boldsymbol{b}_B+\boldsymbol{a}_i+\sum_{j=1}^{i-1}(\boldsymbol{a}_j+\boldsymbol{b}_j)\right]\right\}\\&\quad+\textstyle\sum_{i=1}^{n}\Delta\dot{\theta}_i\times\left[\sum_{j=i}^{n}m_j(\boldsymbol{a}_j+\sum_{k=i}^{j-1}(\boldsymbol{a}_k+\boldsymbol{b}_k))\right]\end{aligned} \tag{38}$$

$$\begin{aligned}\widetilde{\boldsymbol{L}}_K&=-\boldsymbol{I}_B\omega_B-\sum_{i=1}^{n}\boldsymbol{I}_i\omega_i-m_B\dot{\boldsymbol{r}}_B\times(\boldsymbol{b}_B+\sum_{i=1}^{n}(\boldsymbol{a}_i+\boldsymbol{b}_i))\\&\quad-\sum_{i=1}^{n}m_i\dot{\boldsymbol{r}}_i\times(\boldsymbol{L}_i)\\&\quad-(\boldsymbol{I}_B+\textstyle\sum_{i=1}^{n}\boldsymbol{I}_i)\Delta\omega_B-\sum_{i=1}^{n}\left[\left(\boldsymbol{I}_i+\sum_{j=i+1}^{n}\boldsymbol{I}_j\right)\Delta\dot{\theta}_i\right]\\&\quad-m_B\Delta\dot{\boldsymbol{r}}_B\times(\boldsymbol{b}_B+\textstyle\sum_{i=1}^{n}(\boldsymbol{a}_i+\boldsymbol{b}_i))\\&\quad-\textstyle\sum_{i=1}^{n}\left[m_i\Delta\dot{\boldsymbol{r}}_i\times(\boldsymbol{b}_i+\sum_{j=i+1}^{n}(\boldsymbol{a}_j+\boldsymbol{b}_j))\right]\\&=\boldsymbol{L}_K-(\boldsymbol{I}_B+\textstyle\sum_{i=1}^{n}\boldsymbol{I}_i)\Delta\omega_B-\sum_{i=1}^{n}\left[\left(\boldsymbol{I}_i+\sum_{j=i+1}^{n}\boldsymbol{I}_j\right)\Delta\dot{\theta}_i\right]\\&\quad-m_B\Delta\dot{\boldsymbol{r}}_B\times(\boldsymbol{b}_B+\textstyle\sum_{i=1}^{n}(\boldsymbol{a}_i+\boldsymbol{b}_i))\\&\quad-\textstyle\sum_{i=1}^{n}\left[m_i\Delta\dot{\boldsymbol{r}}_i\times(\boldsymbol{b}_i+\sum_{j=i+1}^{n}(\boldsymbol{a}_j+\boldsymbol{b}_j))\right]\end{aligned} \tag{39}$$

Comparing Eqs. (34)–(35) and (38)–(39) with Eqs. (23)–(26), the errors $\Delta\omega_U$, $\Delta\dot{\boldsymbol{p}}_U$, $\Delta\boldsymbol{P}_K$ and $\Delta\boldsymbol{L}_K$ from Eqs. (23)–(26) can be induced and formed by Eqs. (40)–(43) as follows, respectively.

$$\Delta\omega_U=\Delta\omega_B+\sum_{i=1}^{n}\Delta\dot{\theta}_i \tag{40}$$

$$\begin{aligned}\Delta\dot{\boldsymbol{p}}_U&=\Delta\dot{\boldsymbol{p}}_B+\Delta\omega_B\times\left[\boldsymbol{a}_B+\boldsymbol{b}_B+\sum_{j=1}^{n}(\boldsymbol{a}_j+\boldsymbol{b}_j)\right]\\&\quad+\sum_{j=1}^{n}\left[\Delta\dot{\theta}_j\times\sum_{k=j}^{n}(\boldsymbol{a}_k+\boldsymbol{b}_k)\right]\end{aligned} \tag{41}$$

$$\begin{aligned}\Delta\boldsymbol{P}_K&=(m_B+\textstyle\sum_{i=1}^{n}m_i)\Delta\dot{\boldsymbol{p}}_B+\Delta\omega_B\times\\&\quad\left\{m_B\boldsymbol{a}_B+\textstyle\sum_{i=1}^{n}m_i\left[\boldsymbol{a}_B+\boldsymbol{b}_B+\boldsymbol{a}_i+\sum_{j=1}^{i-1}(\boldsymbol{a}_j+\boldsymbol{b}_j)\right]\right\}\\&\quad+\textstyle\sum_{i=1}^{n}\Delta\dot{\theta}_i\times\left[\sum_{j=i}^{n}m_j(\boldsymbol{a}_j+\sum_{k=i}^{j-1}(\boldsymbol{a}_k+\boldsymbol{b}_k))\right]\end{aligned} \tag{42}$$

$$\begin{aligned}\Delta\boldsymbol{L}_K&=-(\boldsymbol{I}_B+\textstyle\sum_{i=1}^{n}\boldsymbol{I}_i)\Delta\omega_B-\sum_{i=1}^{n}\left[\left(\boldsymbol{I}_i+\sum_{j=i+1}^{n}\boldsymbol{I}_j\right)\Delta\dot{\theta}_i\right]\\&\quad-m_B\Delta\dot{\boldsymbol{r}}_B\times(\boldsymbol{b}_B+\textstyle\sum_{i=1}^{n}(\boldsymbol{a}_i+\boldsymbol{b}_i))\\&\quad-\textstyle\sum_{i=1}^{n}\left[m_i\Delta\dot{\boldsymbol{r}}_i\times(\boldsymbol{b}_i+\sum_{j=i+1}^{n}(\boldsymbol{a}_j+\boldsymbol{b}_j))\right]\\&\Delta\dot{\boldsymbol{r}}_B=\Delta\dot{\boldsymbol{p}}_B+\Delta\omega_B\times\boldsymbol{a}_B\\&\Delta\dot{\boldsymbol{r}}_i=\Delta\dot{\boldsymbol{p}}_B+\Delta\omega_B\times\left[\boldsymbol{a}_B+\boldsymbol{b}_B+\textstyle\sum_{j=1}^{i-1}(\boldsymbol{a}_j+\boldsymbol{b}_j)+\boldsymbol{a}_i\right]\\&\quad+\textstyle\sum_{j=1}^{i}\Delta\dot{\theta}_j\times\left[\boldsymbol{a}_j+\sum_{k=j}^{i-1}(\boldsymbol{b}_k+\boldsymbol{a}_{k+1})\right]\end{aligned} \tag{43}$$

The above Eqs. (40)–(43) show that the errors of the coefficient matrixes or vectors ($\Delta\omega_U$, $\Delta\dot{\boldsymbol{p}}_U$, $\Delta\boldsymbol{P}_K$, $\Delta\boldsymbol{L}_K$) are gradually accumulated from the measurement errors $\Delta\dot{\boldsymbol{p}}_B$, $\Delta\omega_B$ and $\Delta\dot{\theta}_i$ (even in a faint way), with the increase of the legends ($\boldsymbol{a}_i$, $\boldsymbol{b}_i$) and amounts (n) of links from the spacecraft to end-effector and also the ideal inertial properties of the spacecraft and manipulator. The measurement errors $\Delta\dot{\boldsymbol{p}}_B$, $\Delta\omega_B$ and $\Delta\dot{\theta}_i$ cannot be completely eliminated in the practical scenario, and the errors of $\Delta\omega_U$,$\Delta\dot{\boldsymbol{p}}_U$,$\Delta\boldsymbol{P}_K$ and $\Delta\boldsymbol{L}_K$ directly impact the accuracy of the identified parameters of m_U, $\boldsymbol{a}_U$, $\boldsymbol{I}_U$,with accumulated calculation from the spacecraft to end-effector.

Furthermore, compared with $\widetilde{\omega}_B$ and $\widetilde{\dot{\boldsymbol{p}}}_B$ measured by the rate gyroscopes and accelerometer installed on the spacecraft, $\widetilde{\dot{\theta}}_i$ needs measured information of the encoder mounted on joint i, with digital signals of smooth output. And compared with $\Delta\omega_B$ and $\Delta\dot{\boldsymbol{p}}_B$, $\Delta\dot{\theta}_i$ has little effect in Eqs. (40)–(43). Then, ignoring the effect of $\Delta\dot{\theta}_i$, one can obtain a group of new equations, (44)–(47), from Eqs. (40)–(43).

$$\Delta\omega_U\approx\Delta\omega_B \tag{44}$$

$$\Delta\dot{\boldsymbol{p}}_U\approx\Delta\dot{\boldsymbol{p}}_B+\Delta\omega_B\times\left[\boldsymbol{a}_B+\boldsymbol{b}_B+\sum_{j=1}^{n}(\boldsymbol{a}_j+\boldsymbol{b}_j)\right] \tag{45}$$

$$\begin{aligned}\Delta\boldsymbol{P}_K&\approx(m_B+\sum_{i=1}^{n}m_i)\Delta\dot{\boldsymbol{p}}_B+\Delta\omega_B\times\\&\quad\left\{m_B\boldsymbol{a}_B+\sum_{i=1}^{n}m_i\left[\boldsymbol{a}_B+\boldsymbol{b}_B+\boldsymbol{a}_i+\sum_{j=1}^{i-1}(\boldsymbol{a}_j+\boldsymbol{b}_j)\right]\right\}\end{aligned} \tag{46}$$

$$\begin{aligned}\Delta L_K \approx &-(I_B + \textstyle\sum_{i=1}^{n} I_i)\Delta\omega_B - m_B\Delta\dot{r}_B \times (b_B + \textstyle\sum_{i=1}^{n}(a_i + b_i))\\ &- \textstyle\sum_{i=1}^{n}\left[m_i\Delta\dot{r}_i \times (b_i + \textstyle\sum_{j=i+1}^{n}(a_j + b_j))\right]\end{aligned}$$

$$\Delta\dot{r}_B = \Delta\dot{p}_B + \Delta\omega_B \times a_B$$

$$\Delta\dot{r}_i = \Delta\dot{p}_B + \Delta\omega_B \times \left[a_B + b_B + \textstyle\sum_{j=1}^{i-1}(a_j + b_j) + a_i\right] \tag{47}$$

From Eqs. (44) and (45), the errors of $\Delta\omega_U$and $\Delta\,\dot{p}_U$ cannot be notably accumulated by resolving the process from the spacecraft to end effector, compared with ΔP_K and ΔL_K containing the accumulations of both the kinematic and inertial properties of the spacecraft and manipulator, which have the greatest distortion impact on the identified inertial parameters of m_U, a_U and I_U.

3. Identification scheme incorporating information of contact force together with force/torque of end-effector

3.1. Modified identification equation

From Eqs. (35) and (38), ΔP_K, $\Delta\,L_K$ and $\Delta\,\dot{p}_U$ could be accumulated by the measurement errors of $\Delta\,\dot{p}_B$, $\Delta\omega_B$ and $\Delta\dot{\theta}_i$ through accumulated calculation from the spacecraft to the end-effector. In fact, there also exists inertial estimation errors of the spacecraft and manipulator that can be accumulated to the coefficient matrix or vectors of the identification equation in a similar way as the accumulation by measurement errors. Therefore, compared with acquiring coefficient information through indirect deduction from the spacecraft and manipulator, with the error accumulation process introducing more uncertainty, a straightaway mode of measurement without too much accumulated calculation is essential and can improve the identification accuracy. From Eqs. (46) and (47), ΔP_K andΔL_K cause the greatest distortions to the identified inertial parameters, containing accumulated errors of both the kinematic and inertial properties of the spacecraft and manipulator. To reduce the errors of ΔP_K, $\Delta\,L_K$ caused by the accumulated calculation from measurement or estimation errors, a new identification scheme incorporating the contact force together with the force/torque of the end-effector is employed to improve the identification precision, as shown in Fig. 3.

In Fig. 3, f_U, n_U denote the contact force and torque acting on all the contact points of the surface of the unknown object, respectively, and f_n, n_n are the force and torque acting on joint n (end-effector), respectively. f, n denote the resultant force and torque of the unknown object acting on the centroid of the unknown object, and n_E denotes the resultant torque of the end-effector acting on the centroid of the end-effector. In practice, $\tilde{f}_U$, $\tilde{f}_n$ and $\tilde{n}_n$ can be measured by a tactile sensor [20,21] and force/torque sensor, with measurement errors of Δf_U, Δf_n and Δn_n, and $\tilde{n}_U$,$\tilde{n}_E$, $\tilde{f}$ and $\tilde{n}$ can be derived by the Newton-Euler

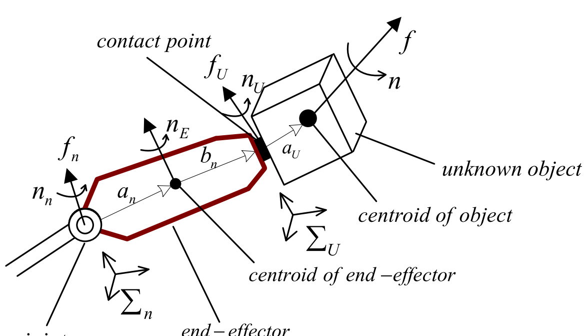

Fig. 3. Force analysis of end-effector.

equation via the acknowledged $I_E$and measured $\tilde{f}_U$, $\tilde{f}_n$ and $\tilde{n}_n$. The derivation process is presented as Eqs. (48)–(51).

$$\tilde{f} = \tilde{f}_U \tag{48}$$

$$\tilde{n} = \tilde{n}_U - a_U \times \tilde{f}_U \tag{49}$$

$$\tilde{n}_U = \tilde{n}_n - \tilde{n}_E - a_n \times \tilde{f}_n - b_n \times \tilde{f}_U \tag{50}$$

$$\begin{aligned}\tilde{n}_E &= I_E\,\dot{\tilde{\omega}}_E + \tilde{\omega}_E \times (I_E\,\tilde{\omega}_E)\\ \tilde{\omega}_E &= \tilde{\omega}_U = \tilde{\omega}_n\end{aligned} \tag{51}$$

After acquiring the essential information of the force and torque from Eqs. (48)–(51), a modified identification equation can be constructed as follows.

From Eqs. (10)–(11) and (13) and (14), the momentum of system can be decomposed by Eqs. (52) and (53),

$$\begin{aligned}\tilde{P} &= \tilde{P}_K + \tilde{P}_U\\ \tilde{P}_U &= m_U\tilde{\dot{r}}_U\end{aligned} \tag{52}$$

$$\begin{aligned}\tilde{L} &= -\tilde{L}_K + \tilde{L}_U + \tilde{P}_K \times a_U\\ \tilde{L}_U &= I_U\tilde{\omega}_U\end{aligned} \tag{53}$$

where $\tilde{P}_U$ and $\tilde{L}_U$ denote the actual linear and angular momentums of the unknown object with errors, respectively, expressed in the inertial frame. Using the conservation of momentum in the robotic system, derivative forms of (52) and (53) can be acquired as Eqs. (54) and (55), respectively.

$$\begin{aligned}\frac{d\tilde{P}}{dt} &= \frac{d\tilde{P}_K}{dt} + \frac{d\tilde{P}_U}{dt} = 0\\ \frac{d\tilde{P}_U}{dt} &= -\frac{d\tilde{P}_K}{dt}\end{aligned} \tag{54}$$

$$\begin{aligned}\frac{d\tilde{L}}{dt} &= -\frac{d\tilde{L}_K}{dt} + \frac{d\tilde{L}_U}{dt} + \frac{d(\tilde{P}_K \times a_U)}{dt} = 0\\ \frac{d\tilde{L}_U}{dt} &= \frac{d\tilde{L}_K}{dt} - \frac{d(\tilde{P}_K \times a_U)}{dt}\end{aligned} \tag{55}$$

Using the momentum theorem, one can obtain Eq. (56) and the integrated form of (56) over a period of δt, i.e., Eq. (57), in which $\tilde{f}$ and $\tilde{n}$ can be acquired by Eqs. (48)–(51). From Eq. (57), $\delta\,\tilde{P}_U$ and $\delta\,\tilde{L}_U$ denote the increments of $\tilde{P}_U$and $\tilde{L}_U$ in the period of δt, respectively.

$$\begin{aligned}d\,\tilde{P}_U &= \tilde{f}\cdot dt\\ d\,\tilde{L}_U &= \tilde{n}\cdot dt\end{aligned} \tag{56}$$

$$\begin{aligned}\delta\,\tilde{P}_U &= \int_0^{\delta t}\tilde{f}\cdot dt\\ \delta\,\tilde{L}_U &= \int_0^{\delta t}\tilde{n}\cdot dt\end{aligned} \tag{57}$$

Hence, by combining Eqs. (54)–(57), one can realize Eqs. (58) and (59), in which the $\delta\tilde{P}_K$ and $\delta\tilde{L}_K$ denote the increments of $\tilde{P}_K$ and $\tilde{L}_K$ in the period of δt, respectively.

$$\begin{aligned}d\tilde{P}_K &= -\tilde{f}\cdot dt\\ d\tilde{L}_K - d(\tilde{P}_K \times a_U) &= d\tilde{L}_K - d(\tilde{P}_K^{\times}\cdot a_U) = \tilde{n}\cdot dt\end{aligned} \tag{58}$$

$$\begin{aligned}\delta\tilde{P}_K &= -\int_0^{\delta t}\tilde{f}\cdot dt\\ \delta\tilde{L}_K - \delta(\tilde{P}_K \times a_U) &= \delta\tilde{L}_K - \delta(\tilde{P}_K^{\times}\cdot a_U) = \int_0^{\delta t}\tilde{n}\cdot dt\end{aligned} \tag{59}$$

Based on the incremental MC method [9,10] to avoid considering the initial momentum of the system, the conventional identification Eqs. (21) and (22) can be replaced by Eqs. (60) and (61), also in a period of δt, and $\delta\tilde{\dot{p}}_U$and$\delta\tilde{\omega}_U$ similarly denote the increments of $\tilde{\dot{p}}_U$and $\tilde{\omega}_U$respectively. By combining Eqs. (59)–(61), a modified linear identification equation is presented by Eqs. (62) and (63).

$$-\;\delta\tilde{\dot{p}}_U = \delta\tilde{P}_K\cdot\frac{1}{m_U} + [(\delta\tilde{\omega}_U)^{\times}]\cdot a_U \tag{60}$$

$$\delta\widetilde{\boldsymbol{L}}_{\boldsymbol{K}} - \delta([\widetilde{\boldsymbol{P}}_{\boldsymbol{K}}^{\times}]\cdot\boldsymbol{a}_U) = [\#(\delta\widetilde{\boldsymbol{\omega}}_U)]\cdot[\boldsymbol{I}_U^{\#}] \tag{61}$$

$$-\delta\,\widetilde{\boldsymbol{p}}_U = -\int_0^{\delta t}\widetilde{\boldsymbol{f}}\cdot dt\cdot\frac{1}{m_U} + [(\delta\widetilde{\boldsymbol{\omega}}_U)^{\times}]\cdot\boldsymbol{a}_U \tag{62}$$

$$\int_0^{\delta t}\widetilde{\boldsymbol{n}}\cdot dt = [\#(\delta\widetilde{\boldsymbol{\omega}}_U)]\cdot[\boldsymbol{I}_U^{\#}] \tag{63}$$

From Eqs. (62) and (63), compared with the conventional incremental equation Eqs. (60) and (61), the identification scheme incorporating the information of $\widetilde{\boldsymbol{f}}$ and $\widetilde{\boldsymbol{n}}$ eliminates the main distortions of $\Delta\boldsymbol{P}_{\boldsymbol{K}}$ and $\Delta\boldsymbol{L}_{\boldsymbol{K}}$ by substituting the integration of $\widetilde{\boldsymbol{f}}$ and $\widetilde{\boldsymbol{n}}$ for the parts of $\widetilde{\boldsymbol{P}}_{\boldsymbol{K}}$ and $\widetilde{\boldsymbol{L}}_{\boldsymbol{K}}$, which dominate the main components by the accumulated calculation from the spacecraft to end-effector in the identification equation. Therefore, the main disturbances to the accuracy of identified parameters by $\Delta\boldsymbol{P}_{\boldsymbol{K}}$ and $\Delta\boldsymbol{L}_{\boldsymbol{K}}$ become the integration of errors from $\widetilde{\boldsymbol{f}}$ and $\widetilde{\boldsymbol{n}}$, namely, $\int\Delta\boldsymbol{f}$ and $\int\Delta\boldsymbol{n}$, respectively. The effect of errors from $\Delta\boldsymbol{f}$ and $\Delta\,\boldsymbol{n}$ on the identification is presented as follows.

Based on Eqs. (48)–(51), Eqs. (62) and (63) can be replaced by Eqs. (64) and (65), and one can also define the errors of the coefficient vectors of $\int\Delta\boldsymbol{f}$ and $\int\Delta\boldsymbol{n}$ by Eqs. (66) and (67).

$$\begin{aligned}-\delta\,\widetilde{\boldsymbol{p}}_U &= -\delta\,(\dot{\boldsymbol{p}}_U + \Delta\dot{\boldsymbol{p}}_U) = -\int_0^{\delta t}\widetilde{\boldsymbol{f}}\cdot dt\cdot\tfrac{1}{m_U} + [(\delta\widetilde{\boldsymbol{\omega}}_U)^{\times}]\cdot\boldsymbol{a}_U\\ &= -\int_0^{\delta t}(\boldsymbol{f}_U + \Delta\boldsymbol{f}_U)\cdot dt\cdot\tfrac{1}{m_U} + [(\delta(\boldsymbol{\omega}_U + \Delta\boldsymbol{\omega}_U))^{\times}]\cdot\boldsymbol{a}_U\\ &= -\left(\int_0^{\delta t}\boldsymbol{f}_U\cdot dt + \int_0^{\delta t}\Delta\boldsymbol{f}_U\cdot dt\right)\cdot\tfrac{1}{m_U} + [(\delta(\boldsymbol{\omega}_U + \Delta\boldsymbol{\omega}_U))^{\times}]\cdot\boldsymbol{a}_U\end{aligned} \tag{64}$$

$$\begin{aligned}\int_0^{\delta t}\widetilde{\boldsymbol{n}}\cdot dt &= \int_0^{\delta t}((\boldsymbol{n}_n + \Delta\boldsymbol{n}_n) - \boldsymbol{a}_n\times(\boldsymbol{f}_n + \Delta\boldsymbol{f}_n)\\ &\quad - (\boldsymbol{b}_n + \boldsymbol{a}_U)\times(\boldsymbol{f}_U + \Delta\boldsymbol{f}_U))\ dt\\ &\quad - \boldsymbol{I}_E\,(\boldsymbol{\omega}_U + \Delta\boldsymbol{\omega}_U)\\ &= \int_0^{\delta t}(\boldsymbol{n}_n - \boldsymbol{a}_n\times\boldsymbol{f}_n - (\boldsymbol{b}_n + \boldsymbol{a}_U)\times\boldsymbol{f}_U)\ dt\\ &\quad + \int_0^{\delta t}(\Delta\boldsymbol{n}_n - \boldsymbol{a}_n\times\Delta\boldsymbol{f}_n - (\boldsymbol{b}_n + \boldsymbol{a}_U)\times\Delta\boldsymbol{f}_U)\ dt - \boldsymbol{I}_E\cdot\boldsymbol{\omega}_U - \boldsymbol{I}_E\cdot\Delta\boldsymbol{\omega}_U\\ &= [\#(\delta(\boldsymbol{\omega}_U + \Delta\boldsymbol{\omega}_U))]\cdot[\boldsymbol{I}_U^{\#}]\end{aligned} \tag{65}$$

$$\int\Delta\boldsymbol{f} = \int_0^{\delta t}\Delta\boldsymbol{f}_U\cdot dt \tag{66}$$

$$\int\Delta\boldsymbol{n} = \int_0^{\delta t}(\Delta\boldsymbol{n}_n - \boldsymbol{a}_n\times\Delta\boldsymbol{f}_n - (\boldsymbol{b}_n + \boldsymbol{a}_U)\times\Delta\boldsymbol{f}_U)\ dt - \boldsymbol{I}_E\cdot\Delta\boldsymbol{\omega}_U \tag{67}$$

From Eqs. (66) and (67), compared with $\Delta\boldsymbol{P}_{\boldsymbol{K}}$ and $\Delta\boldsymbol{L}_{\boldsymbol{K}}$ from Eqs. (46) and (47), which incorporate the accumulated kinematic measurement errors from $\Delta\,\dot{\boldsymbol{p}}_{\boldsymbol{B}}$, $\Delta\boldsymbol{\omega}_B$, $\Delta\dot{\boldsymbol{\theta}}_i$ and the inertial estimation errors from the inertial properties of the spacecraft and manipulator, $\int\Delta\boldsymbol{f}$ and $\int\Delta\boldsymbol{n}$ are only affected by the measurement errors of $\Delta\boldsymbol{f}_U$, $\Delta\boldsymbol{f}_n$, $\Delta\boldsymbol{n}_n$ and not notably by the accumulated error of $\Delta\boldsymbol{\omega}_U$, via the faint accumulated process with $\boldsymbol{a}_n$, $\boldsymbol{b}_n$, $\boldsymbol{I}_E$ and identified $\boldsymbol{a}_U$ from joint n to the unknown object. Therefore, the main distinction between the conventional identification scheme from Eqs. (60) and (61) and the proposed identification scheme incorporating the information of $\widetilde{\boldsymbol{f}}_U$,$\widetilde{\boldsymbol{f}}_n$ and $\widetilde{\boldsymbol{n}}_n$ from Eqs. (62) and (63) is that the proposed scheme weakens the process of accumulated calculation with "direct" measured information of $\widetilde{\boldsymbol{f}}_U$,$\widetilde{\boldsymbol{f}}_n$ and $\widetilde{\boldsymbol{n}}_n$ and thereby improves the accuracy of identification. The residual errors of the modified identification equation are $\Delta\,\dot{\boldsymbol{p}}_U$, $\Delta\,\boldsymbol{\omega}_U{}^{\times}$and $\#\Delta\boldsymbol{\omega}_U$ from Eqs. (62) and (63), whereas the errors of $\Delta\boldsymbol{\omega}_U$ and $\Delta\,\dot{\boldsymbol{p}}_U$ cannot be significantly accumulated from Eqs. (44) and (45). Therefore, the modified identification presents improved accuracy by incorporating the contact force and the force/torque of the end-effector.

There exist two crucial considerations for the practical scenario:

(1) The error analysis considered in this section is in the inertial coordinate frame by all the vectors and matrixes to simplify the expressions of the analysis process. In fact, the measured data of the contact force and the force/torque of the end-effector are always obtained and expressed in the body coordinate frames of Σ_U and Σ_n, respectively. The rotation matrix converting vector expressions from various coordinate frames into the identical frame is needed for the composition of vectors. Therefore, there is also a need for the Euler angles $(\widetilde{\varphi}, \widetilde{\psi}, \widetilde{\eta})$ of the spacecraft's attitude and the driven angles $\widetilde{\boldsymbol{\theta}}_i$ of all joints to construct essential rotation matrixes, and the errors of the rotation matrixes are inevitably introduced into the identification process, also in the conventional identification scheme. Hence, how to reduce the error effect of the rotation matrix on the identification process is still a problem to be solved.

(2) The integrations in Eqs. (62) and (63) require continuous-time signals of $\boldsymbol{f}$ and $\boldsymbol{n}$, which is impossible in a discrete state of the measuring process. In practice, the integral of the force and torque can be approximated from a known time history in a period of$\delta t$from Eqs. (62) and (63), and the integration method and also the sampling rate of γ from Eq. (68) dominate the accuracy of the terms by integration, e.g., the implicit trapezoid method. From the integration method, a lower γ is superior to the integral process, which means a longer period ofδt for the inherent sampling frequency of sensors by force or torque. However, from Eqs. (66) and (67), the integral errors produced by the measurement errors of $\Delta\boldsymbol{f}_U$, $\Delta\boldsymbol{f}_n$, $\Delta\boldsymbol{n}_n$ will be increased with a long period of δt, which directly leads to a larger deviation by the errors of $\int\Delta\boldsymbol{f}$ and $\int\Delta\boldsymbol{n}$ and thus influences the accuracy of the identified parameters. Therefore, a suitable δt is employed to improve the accuracy of identification.

$$\gamma = \frac{\tau_{f,n}}{\delta t}\ (\text{:sampling period of force and torque information}) \tag{68}$$

3.2. Solution of the modified identification equation using the hybrid RLS-APSA algorithm

From (62) and (63) of the modified identification equation, one can construct linear regression forms of Eqs. (69) and (70). Eqs. (69) and (70) can be simplified into the form of a linear equation as (71). In Eq. (71),$\boldsymbol{\theta}$ denotes the vectors composed of the unknown inertial parameters to be identified, and $\boldsymbol{A}$ and $\boldsymbol{b}$ denote the coefficient matrix and vector of the identification equation, respectively.

$$\begin{aligned}&\boldsymbol{A}_1\boldsymbol{\theta}_1 = \boldsymbol{b}_1\\ &\boldsymbol{A}_1 = \left[-\int_0^{\delta t}\boldsymbol{f}_U\cdot dt \qquad [(\delta\boldsymbol{\omega}_U)^{\times}]\right] \qquad \boldsymbol{b}_1 = -\delta\,\dot{\boldsymbol{p}}_U \qquad \boldsymbol{\theta}_1 = \begin{bmatrix}\frac{1}{m_U}\\ \boldsymbol{a}_U\end{bmatrix}\end{aligned} \tag{69}$$

$$\begin{aligned}&\boldsymbol{A}_2\,\boldsymbol{\theta}_2 = \boldsymbol{b}_2\\ &\boldsymbol{A}_2 = [\#(\delta\boldsymbol{\omega}_U)] \qquad \boldsymbol{b}_2 = \int_0^{\delta t}(\boldsymbol{n}_n - \boldsymbol{a}_n\times\boldsymbol{f}_n - \boldsymbol{b}_n\times\boldsymbol{f}_U - \boldsymbol{a}_U\times\boldsymbol{f}_U)\ dt - \boldsymbol{I}_E\,\boldsymbol{\omega}_U \qquad \boldsymbol{\theta}_2 = [\boldsymbol{I}_U^{\#}]\end{aligned} \tag{70}$$

$$\boldsymbol{A}\ \boldsymbol{\theta}\ = \boldsymbol{b} \tag{71}$$

In Eqs. (69) and (70), the singular linear equation needs to be resolved by constructing normal or overdetermined equations through multi-set coefficient matrices (A, b) that are gathered by the kinematics of various moments from the robotic system. A linear regression

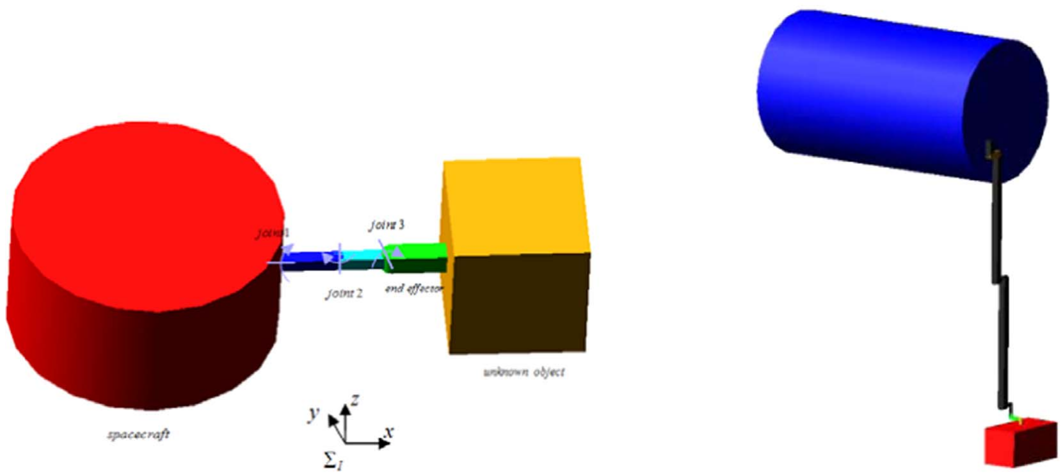

(a) Space robotic system model with 3-DOF manipulator (b) Space robotic system model with 7-DOF manipulator

Fig. 4. Dynamic model of space robotic system.

algorithm or an adaptive filter algorithm is adopted to resolve the modified identification equation in Eq. (71). Conventional identification schemes use the LS (Least Squares) or RLS (Recursive Least Squares) algorithm to obtain the identification results. However, the LS or RLS cannot address the coloured noise or intense spike pulse noise that occurs in practice. To solve this problem, a hybrid algorithm [22–24] is introduced by combining the RLS and APSA (Affine Projection Sign Algorithm). The RLS maintains the speed and reduces the correlation of measured data [25], which can rapidly obtain approximate results for identified parameters with a high computation complexity, and the APSA (affine projection sign algorithm) [26] is immune to coloured noise and impulse noise and also has a low computation complexity but maintains a slow rate of convergence. The standard regression forms of RLS and APSA are presented by Eqs. (72) and (73), respectively.

$$\begin{aligned}\hat{\boldsymbol{\theta}}_{(k+1)} &= \hat{\boldsymbol{\theta}}_{(k)} + \boldsymbol{K}_{(k+1)}[\,\boldsymbol{b}_{(k+1)} - \boldsymbol{A}_{(k+1)}\hat{\boldsymbol{\theta}}_{(k)}] \\ \boldsymbol{K}_{(k+1)} &= \frac{\boldsymbol{P}_{(k)}\boldsymbol{A}_{(k+1)}}{\lambda \boldsymbol{I} + \boldsymbol{A}_{(k+1)}^{\mathrm{T}}\boldsymbol{P}_{(k)}\boldsymbol{A}_{(k+1)}} \\ \boldsymbol{P}_{(k+1)} &= \frac{1}{\lambda}\,[\,\boldsymbol{I} - \boldsymbol{K}_{(k+1)}\boldsymbol{A}_{(k+1)}^{\mathrm{T}}]\,\boldsymbol{P}_{(k)}\end{aligned} \tag{72}$$

$$\begin{aligned}\hat{\boldsymbol{\theta}}_{(k+1)} &= \hat{\boldsymbol{\theta}}_{(k)} + \mu\frac{\boldsymbol{X}_{(k)}\mathrm{sgn}(\boldsymbol{E}_{(k)})}{\sqrt{\mathrm{sgn}(\boldsymbol{E}^{T}{}_{(k)})\cdot \boldsymbol{X}_{(k)}\cdot \boldsymbol{X}^{T}{}_{(k)}\cdot \mathrm{sgn}(\boldsymbol{E}_{(k)}) + \varepsilon}} \\ \boldsymbol{X}_{(k)} &= [\boldsymbol{A}_{(k)}\ ;\ \boldsymbol{A}_{(k-1)}\ ;\ \boldsymbol{A}_{(k-2)}\ \ldots\ \boldsymbol{A}_{(k-M+1)}\,] \\ \boldsymbol{E}_{(k)} &= \boldsymbol{b}_{(k)} - \boldsymbol{X}^{T}{}_{(k)}\cdot\boldsymbol{\theta}_{(k)}\end{aligned} \tag{73}$$

In Eqs. (72) and (73), $\boldsymbol{A}_{(k)}$, $\boldsymbol{b}_{(k)}$ are the coefficient matrix and vector of A, b from Eq. (71), respectively, measured at the kth moment from the robotic system, and $\hat{\boldsymbol{\theta}}_{(k)}$ is an estimate of $\boldsymbol{\theta}$ from (71) at iteration k. From Eq. (72), the forgetting factor λ adjusts the rate of convergence and weakens the effect of the previous data information [25]. In Eq. (73), the step-size parameter μ and the regularization parameter ε (a small positive number) adjust the convergence rate of APSA, and M denotes the Mth previous moment from moment k. The RLS algorithm contains matrix inversion from matrix K in Eq. (72), which is replaced by a square root operation of a positive number from APSA to decrease the complexity of the calculation.

To combine the RLS and APSA during the process of identification, a switching mechanism to detect and decide when to switch between RLS and APSA is needed. Inspired by [24], the switching mechanismcan be achieved by Eq. (74).

$$\left|\frac{d}{dt}\|\boldsymbol{e}_{(k)}\|_2^2\right| \underset{<}{\overset{\geq}{}} APSA^{\ RLS}\ \rho_0 \tag{74}$$

where

$$\boldsymbol{e}_{(k)} = \boldsymbol{b}_{(k+1)} - \boldsymbol{A}_{(k+1)}\hat{\boldsymbol{\theta}}_{(k)} \tag{75}$$

In Eq. (74), ρ_0 is the detection threshold for the change rate of errors from Eq. (75), which determines the algorithm used for identification in the current status. Generally, the RLS algorithm will initially converge quickly and can be used in the initial process of identification. Once it has converged with a gradually slowing rate due to the accumulated noise, the estimated $\hat{\boldsymbol{\theta}}_{(k)}$ changes slowly, and the change rate of the norm of $\boldsymbol{e}_{(k)}$ can be slower than that ofρ_0, so one can switch over to the APSA to continue converging at a slower rate, maintaining the stability of the identification process via the immune performance for coloured noise and impulsive noise. Therefore, the decision to choose the algorithm is based on the threshold ρ_0, by the change rate of $\boldsymbol{e}_{(k)}$. One can also obtain the relationship by Eq.(76), in which the ρ_1 denotes the threshold of the change rate of the identified parameters.

$$|\,\|\hat{\boldsymbol{\theta}}(k+1) - \hat{\boldsymbol{\theta}}(k)\|_2^2| \underset{<}{\overset{\geq}{}} APSA^{\ RLS}\ \rho_1 \tag{76}$$

It is important to note that μ from Eq. (73) controls the convergence level of the APSA, and it should be much smaller than 1 to guarantee the convergence during the identification process [26]; it can be set in the range of (0,1] to achieve a small steady-state misalignment. The deviation $|\hat{\boldsymbol{\theta}}(k) - \boldsymbol{\theta}(k)|$ also maintains an upper bound proportional to $(1-\lambda)$ from constant $\lambda \in (0,1]$ and increases with the data correlation of $(\boldsymbol{A}_{(k)},\boldsymbol{b}_{(k)})$ [25]. Hence, one should decrease the value of $(1-\lambda)$ to maintain the deviation below an admissible level and ensure convergence. As a result, a faster convergence of tge identification process can be realized by using the RLS from the beginning, with a suitable constant λ from (0,1], and the end of the convergence of the RLS induces the change of the algorithm by switching from RLS to APSA to maintain an immune and stable performance in the identification process, with a much smaller μ.

4. Numerical simulation

To verify the validity of the identification method proposed in this paper, a simplified dynamic model of a space robotic system with a manipulator (3-DOF/7-DOF) is established by ADAMS, with orthogonal joints installed on the manipulator, as depicted in Fig. 4. The geometric and inertial parameters of the space robot model are displayed in Tables 1 and 2, expressed in the body frame of all the parts of the robotic system. The robotic system maintains a zero-momentum initial condition, with the initial linear or angular velocity of all the parts of the robotic system maintained at zero. To ensure the

Table 1
Geometric and inertial parameters of space robot model with 3-DOF manipulator.

Link i	Mass/kg m_i	Length/m						Inertia tensor/kg m^2					
		a_i			b_i			$I_i(1,1)$	$I_i(2,2)$	$I_i(3,3)$	$I_i(1,2)$	$I_i(1,3)$	$I_i(2,3)$
0	1000.0	0.0	0.0	0.0	1.0	0.0	0.0	1000.00	1000.00	500.00	0	0	0
1	5.0	0.2	0.0	0.0	0.2	0.0	0.0	0.10	0.10	0.05	0	0	0
2	10.0	0.2	0.0	0.0	0.2	0.0	0.0	0.10	0.20	0.20	0	0	0
3	5.0	0.2	0.0	0.0	0.2	0.0	0.0	0.10	0.10	0.05	0	0	0
Unknown object	100.0	0.5	0.0	0.0	–	–	–	10.00	20.00	10.00	0	0	0

Table 2
Geometric and inertial parameters of space robot model with 7-DOF manipulator.

Link i	Mass/kg m_i	Length/m						Inertia tensor/kg m^2					
		a_i			b_i			$I_i(1,1)$	$I_i(2,2)$	$I_i(3,3)$	$I_i(1,2)$	$I_i(1,3)$	$I_i(2,3)$
0	1606.0	0.0	0.0	0.043	0.135	0.0	0.0	9.05e+2	2.34e+3	2.55e+3	0.00	0.00	0.00
1	6.75	0.0	0.0	0.043	0.135	0.0	0.0	0.028	0.028	0.0116	0.00044	0.00	0.00
2	6.75	0.0	0.0	0.032	0.135	0.0	0.0	0.028	0.028	0.0116	0.00044	0.00	0.00
3	16.5	0.0	0.891	0.041	0.0	0.891	0.139	5.96	5.96	0.609	0.00	0.00	0.2537
4	16.5	0.891	0.0	0.041	0.891	0.0	0.139	5.96	5.96	0.609	0.00	0.00	0.2537
5	6.75	0.0	0.0	0.041	0.0	0.0	0.139	0.028	0.028	0.0116	0.00044	0.00	0.00
6	6.75	0.0	0.0	0.05	0.0	0.0	0.135	0.028	0.028	0.0116	0.00044	0.00	0.00
7	6.57	0.0	0.0	0.045	0.0	0.08	0.0	0.0085	0.0055	0.01	0.00	0.00	0.00
Unknown object	500.0	0.0	-0.25	0.0	–	–	–	100.00	200.00	200.00	0.00	0.00	0.00

Table 3
Actuating signals of joints.

Time/s	Joint 1/		Joint 2/		Joint 3/	
	rad s^{-1}	rad s^{-2}	rad s^{-1}	rad s^{-2}	rad s^{-1}	rad s^{-2}
0	0	$2\pi\cos(\pi t)$	0	$2\pi\cos(\pi t)$	0	$2\pi\cos(\pi t)$
0–100	–	$2\pi\cos(\pi t)$	–	$2\pi\cos(\pi t)$	–	$2\pi\cos(\pi t)$

Table 4
Impulsive noises υ_3.

Time/s	0–30	30	30–35	35	35–40	40	40–55	55	55–100
Impact strength	0	1	0	−0.5	0	1	0	−0.5	0

adequate motion condition for identification from Eq. (18), the orthogonal joints installed on the manipulator were simultaneously driven by cosine signals of acceleration, while maintaining the motion of the robotic system in a period of 100 s in the post-capture phase, as displayed in Table 3. The identification process is implemented by a constructed ADAMS-MATLAB co-simulation platform in an off-line state, with a data sample period τ of 0.005 s and an integration period δt o f 0.1 s, i.e., a sampling rate γ of 0.05.

On account of the severe disturbance condition not solely from Gaussian white noises in space, the measurement errors in the simulation from the Gaussian white noise υ_1, Gaussian coloured noise υ_2 and impulsive noise υ_3 in all measured data must be added, i.e., $(\tilde{\varphi}, \tilde{\psi}, \tilde{\eta}), \tilde{\boldsymbol{p}}_{\boldsymbol{B}}, \tilde{\varpi}_B \tilde{\boldsymbol{f}}_U, \tilde{\boldsymbol{f}}_n, \tilde{\boldsymbol{n}}_n$ ($\Delta\dot{\boldsymbol{\theta}}_i$ is ignored by the digital output of $\tilde{\dot{\boldsymbol{\theta}}}_i$), in which the Gaussian white noise an Gaussian coloured noise are presented by Eqs. (77) and (78), respectively, and the impulsive noise is presented in Table 4. From Eqs. (77) and (78), the random signal x_1(t), x_2(t) has a zero mean value and a standard deviation that is 1% of the signal magnitude.

Considering aerospace operation by fuel consumption, the estimation errors of the prior knowledge of the spacecraft's mass and centroid are 5% of the nominal values in the process of identification [8].

$$v_1 = x_1(t) \tag{77}$$

$$v_2 = x_2(t) + 0.01 \times x_2(t - 0.1) \tag{78}$$

Based on Eqs. (60)–(63), a perfect parameter setting by the algorithm of conventional RLS or RLS-APSA is essential and distinct by identifying the m_U, $\boldsymbol{a}_U$ by Eqs. (60) or (62) and $\boldsymbol{I}_U$ by Eqs. (61) or (63) for the organization form of the coefficient matrix and vector incorporating various kinematic and inertial information. Therefore, a suitable setting is employed in the simulation and presented as Table 5.

Therefore, to compare the advantage from the modified identification with the conventional identification, the comparisons of modified identification and conventional identification with the 3-DOF manipulator via the algorithms of RLS and RLS-APSA are presented in the Fig. 5 and Table 6. Among in, to verify the superior accuracy of the modified identification equation by Eqs. (62) and (63), incorporating the contact force as well as the force/torque of the end-effector, a comparison process is implemented by identifying the inertial parameters of an unknown object using the modified identification Eqs. (62) and (63) and also the conventional identification Eqs. (60) and (61) via the identical algorithm of APSA by parallel parameter setting from Table 5. In addition, to confirm the stability of the identification process resulting from the proposed RLS-APSA, another comparison process is implemented by identifying the inertial parameters using the

Table 5
Parameter settings.

Parameter	λ		μ		ε		M		ρ_1	
	m_U, $\boldsymbol{a}_U$	$\boldsymbol{I}_U$	m_U, $\boldsymbol{a}_U$	$\boldsymbol{I}_U$	m_U, $\boldsymbol{a}_U$	$\boldsymbol{I}_U$	m_U, $\boldsymbol{a}_U$	$\boldsymbol{I}_U$	m_U, $\boldsymbol{a}_U$	$\boldsymbol{I}_U$
Value	0.999	0.9995	0.00001	0.01	1	1	2	2	0.0005	0.01

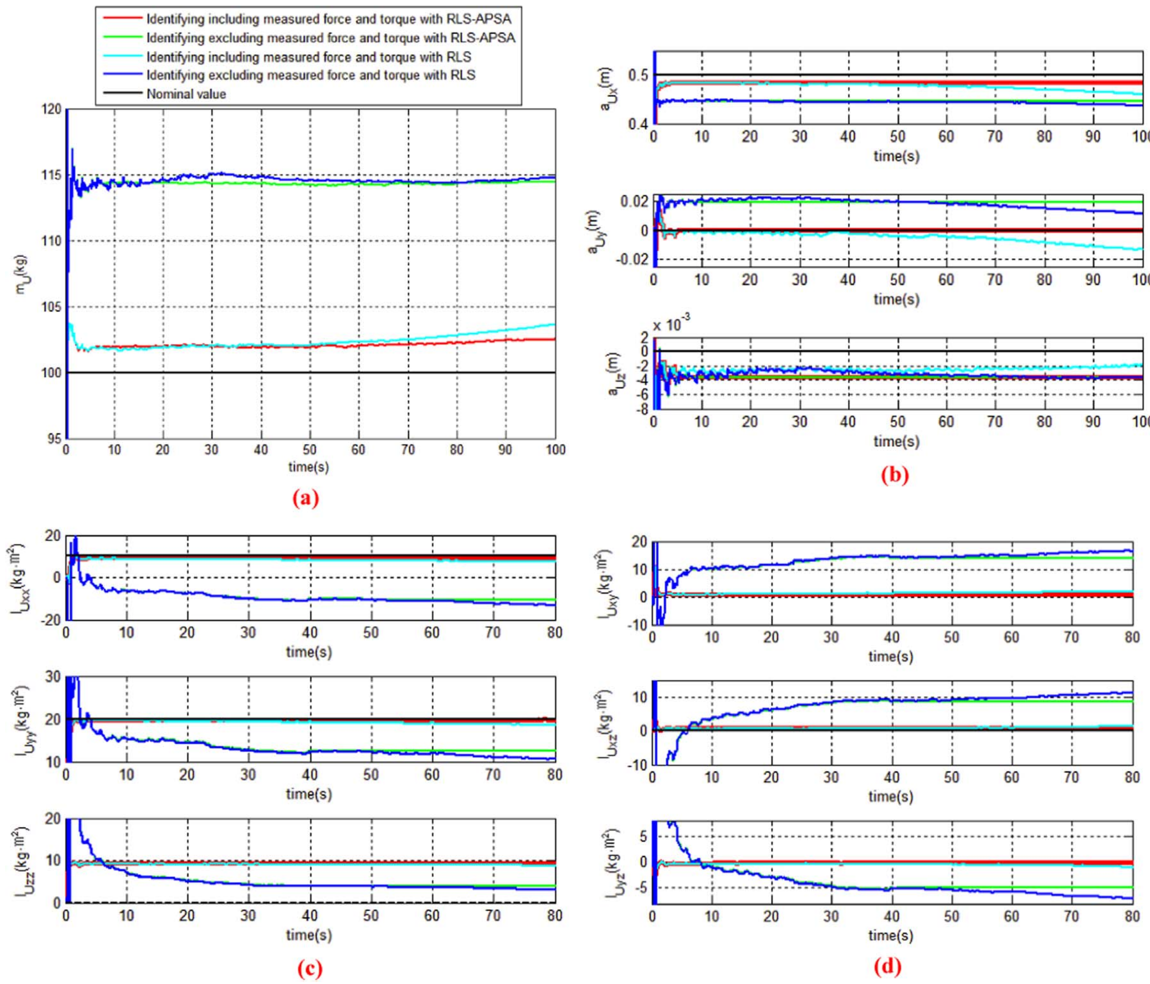

Fig. 5. Comparisons of modified identification and conventional identification via algorithm of RLS and RLS-APSA.

Table 6
Simulation results of modified identification and conventional identification via algorithm of RLS and RLS-APSA.

Inertial parameter	Nominal value	Modified identification method		Conventional identification method	
		Identified mean value(90–100 s)/ Error(%)		Identified mean value (90–100 s)/ Error(%)	
		RLS	RLS-APSA	RLS	RLS-APSA
m_U/kg	100.00	-/-	102.57/ 2.57%	-/-	114.20/ 14.2%
a_{Ux}/m	0.50	-/-	0.485/-3%	-/-	0.452/9.6%
a_{Uy}/m	0.00	-/-	0.002/-	-/-	0.021/-
a_{Uz}/m	0.00	-/-	-0.004/-	-/-	-0.004/-
I_{Uxx}/kg m^2	10.00	-/-	9.82/1.8%	-/-	-9.80/-98%
I_{Uxy}/kg m^2	0.00	-/-	0.50/-	-/-	13.50/-
I_{Uxz}/kg m^2	0.00	-/-	0.12/-	-/-	9.60/-
I_{Uyy}/kg m^2	20.00	-/-	19.85/0.75%	-/-	13.20/34%
I_{Uyz}/kg m^2	0.00	-/-	0.72/-	-/-	-5.01/-
I_{Uzz}/kg m^2	10.00	-/-	9.75/2.5%	-/-	4.8/48%

hybrid RLS-APSA and also conventional RLS via an identical scheme of a modified identification equation by (62) and (63). The attached hybrid measured noises meeting the Eqs. (77) and (78) and Table 4 is followed in the simulation.

From the Fig. 5, the identification scheme incorporating contact force and the force/torque of the end-effector presents notably superior results in identification compared with the conventional scheme via both the algorithm of RLS and RLS-APSA, except that a_{Uy}, a_{Uz} were not clearly distinct. And the RLS-APSA algorithm shows the performance of stability during the process of identification both in modified method and in conventional method, through the various noises including Gaussian white noise, Gaussian coloured noise and impulsive noise. There also exist fluctuations in the identified values in the initial phase of the identification process for both identification schemes and also a break point from fluctuations to a stable process, which is determined by the detection thresholdρ_1 switching the algorithm from RLS to APSA to maintain the stability of the identification process.

Table 7
Rank of Gauss white noise.

Rank	A mean value /standard deviation	B mean value /standard deviation	C mean value /standard deviation
–	0/0.1% of the Signal magnitude	0/1% of the Signal magnitude	0/10% of the Signal magnitude

From Table 6, the identification scheme incorporating the contact force and the force/torque of the end-effectorvia RLS-APSA has major deviations of 2.57% and 1.80% from m_U and I_{Uxx}, compared with the conventional identification scheme having major deviations of 14.20% and −98% from m_U and I_{Uxx}, respectively. Therefore, a remarkable performance improvement in terms of accuracy is achieved by introducing the measured information of the contact force and force/torque of the end-effector into the conventional identification scheme.

Actually, the precision of the tactile sensors and force/torque sensor

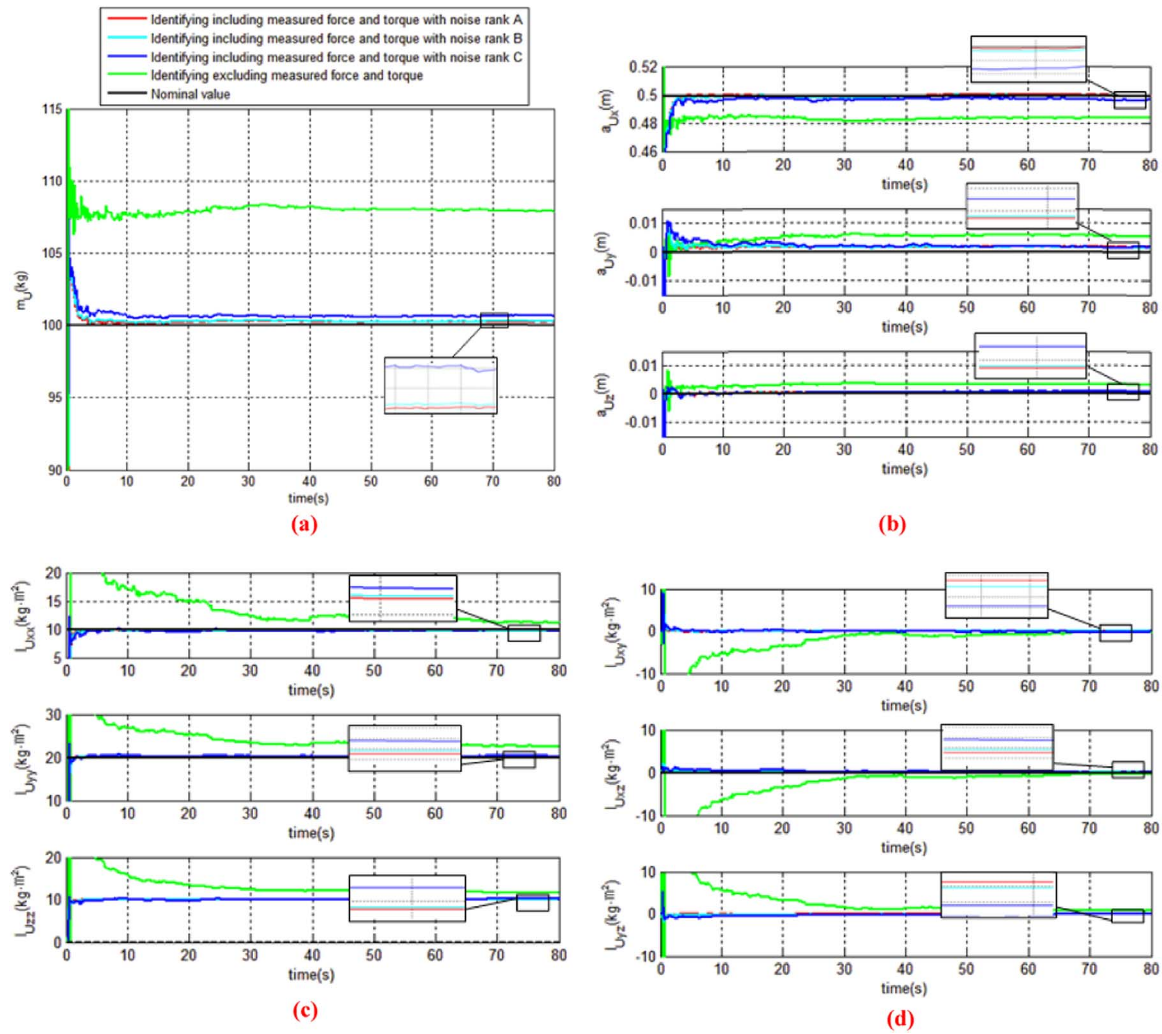

Fig. 6. Comparisons of modified identification via various ranks of measured noises of the force and torque.

Table 8
Simulation results of modified identification via various ranks of measured noises of the force and torque.

Inertial parameter	Nominal value	Modified identification method Identified mean value(70–80 s)/ Error(%) with noise A with noise B with noise C	Conventional identification method Identified mean value (70–80 s) /Error(%)
m_U/kg	100.00	100.94/0.94% 101.23/ 1.23% 102.34/2.34%	107.98/7.98%
a_{Ux}/m	0.50	0.498/-0.4% 0.497/- 0.6% 0.494/-1.2%	0.482/-3.6%
a_{Uy}/m	0.00	0.0017/- 0.0018/- 0.002/-	0.006/-
a_{Uz}/m	0.00	0.00005/- -0.00007/- -0.00009/-	0.0035/-
I_{Uxx}/kg m^2	10.00	10.02/0.2% 10.03/ 0.3% 10.06/0.6%	11.8/18%
I_{Uxy}/kg m^2	0.00	0.12/- 0.13/- 0.15/-	0.2/-
I_{Uxz}/kg m^2	0.00	0.04/- 0.6/- 0.9/-	-0.18/-
I_{Uyy}/kg m^2	20.00	20.2/1% 20.3/1.5% 20.7/3.5%	23.8/16%
I_{Uyz}/kg m^2	0.00	-0.21/- -0.27/- -0.72/-	1.3/-
I_{Uzz}/kg m^2	10.00	10.1/1% 10.15/1,5% 10.35/3.5%	12.1/21%

Table 9
Simulation results of modified identification and conventional identification via algorithm of RLS and RLS-APSA.

Inertial parameter	Nominal value	Modified identification method		Conventional identification method	
		Identified mean value(90–100 s)/ Error(%)		Identified mean value (90–100 s)/Error(%)	
		RLS	RLS-APSA	RLS	RLS-APSA
m_U/kg	500.00	-/-	510.12/ 2.02%	-/-	519.72/3.94%
a_{Ux}/m	0.00	-/-	-0.002/-	-/-	0.026/-
a_{Uy}/m	-0.25	-/-	-0.252/0.8%	-/-	-0.29/16%
a_{Uz}/m	0.00	-/-	0.005/-	-/-	0.023/-
I_{Uxx}/kg m^2	100.00	-/-	101.12/ 1.12%	-/-	162.81/ 62.81%
I_{Uxy}/kg m^2	0.00	-/-	-0.52/-	-/-	-24.58/-
I_{Uxz}/kg m^2	0.00	-/-	-5.71/-	-/-	-26.9/-
I_{Uyy}/kg m^2	200.00	-/-	201.33/ 0.67%	-/-	222.12/ 11.06%
I_{Uyz}/kg m^2	0.00	-/-	3.28/-	-/-	6.45/-
I_{Uzz}/kg m^2	200.00	-/-	200.94/ 0.47%	-/-	145.37/- 27.32%

Table 10
Simulation results of modified identification via various ranks of measured noises of the force and torque.

Inertial parameter	Nominal value	Modified identification method			Conventional identification method
		Identified mean value(70–80 s)/ Error(%)			Identified mean value(70–80 s)/ Error(%)
		With noise A	With noise B	With noise C	
m_U/kg	500.00	503.08/ 0.62%	503.09/ 0.62%	503.11/ 0.63%	504.17/0.83%
a_{Ux}/m	0.00	0.001/-	0.002/-	0.004/-	0.008/-
a_{Uy}/m	-0.25	-0.240/ 4%	-0.239/ 4.4%	-0.237/ 5.2%	-0.230/8%
a_{Uz}/m	0.00	-0.021/-	-0.022/-	-0.0024/-	-0.031/-
I_{Uxx}/kg m^2	100.00	102.02/ 2.02%	102.04/ 2.04%	102.13/ 2.13%	90.8/-9.20%
I_{Uxy}/kg m^2	0.00	-0.12/-	-0.13/-	-0.15/-	2.83/-
I_{Uxz}/kg m^2	0.00	1.12/-	1.10/-	1.31/-	-2.01/-
I_{Uyy}/kg m^2	200.00	202.24/ 1.12%	202.27/ 1.13%	202.35/ 1.18%	203.57/1.79%
I_{Uyz}/kg m^2	0.00	-0.31/-	-0.32/-	-0.37/-	1.13/-
I_{Uzz}/kg m^2	200.00	199.95/- 0.03%	199.92/- 0.04%	199.83/- 0.09%	202.13/1.07%

plays a fundamental role in the modified identification. And to show the identification under various accuracies of tactile sensor and force/torque sensor, the different ranks of Gauss white noises is defined in Table 7 and employed as measured noises in tactile sensor and force/torque sensor in the process of simulation. And from the identified results from Fig. 6 and Table 8, the modified identification including measured force and torque shows the better performance of precision compared to conventional identification. Furthermore, the precision of identified results can be slightly enhanced with the accuracy improvement of measured force and torque. Analogously, the simulated conditions are parallel to the space robotic system with the 7-DOF manipulator, and simultaneously the simulated results are presented in Tables 9 and 10, Figs. 7 and 8. In conclusion, the identification scheme incorporating the measured information of the contact force and the force/torque of the end-effector can significantly overcome the effect of above mentioned accumulated errors caused by accumulative calculation process from spacecraft to the end-effector, and improves the precision of the identification of the inertial parameters, and the proposed hybrid RLS-APSA algorithm effectively ensures the stability of the identification process.

5. Conclusions

An intact inertial parameter identification scheme using contact force information for a space unknown object captured by a manipulator is proposed in this paper, which includes a two-step identification process of mass and centroid estimation and then inertial tensor

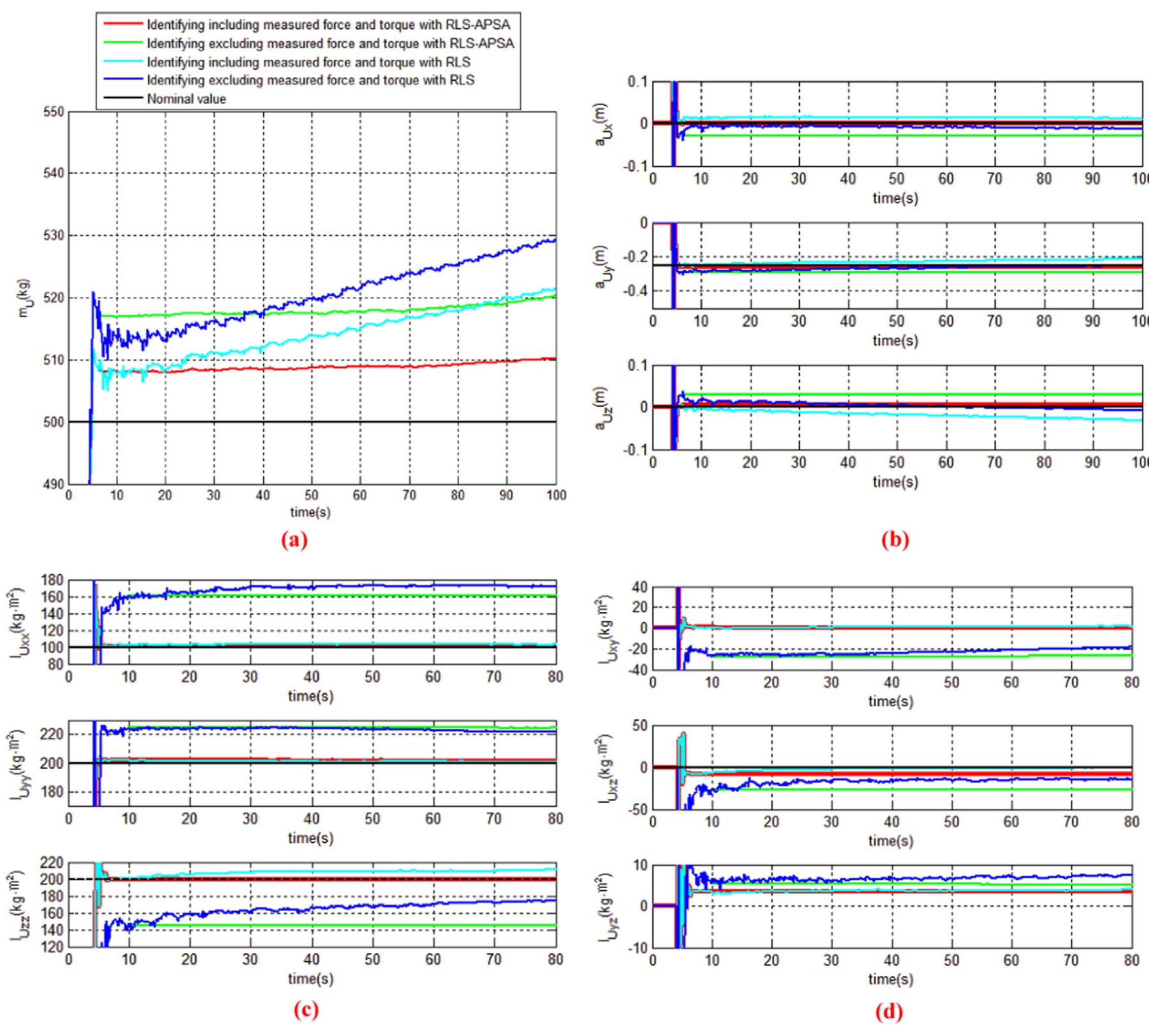

Fig. 7. Comparisons of modified identification and conventional identification via algorithm of RLS and RLS-APSA.

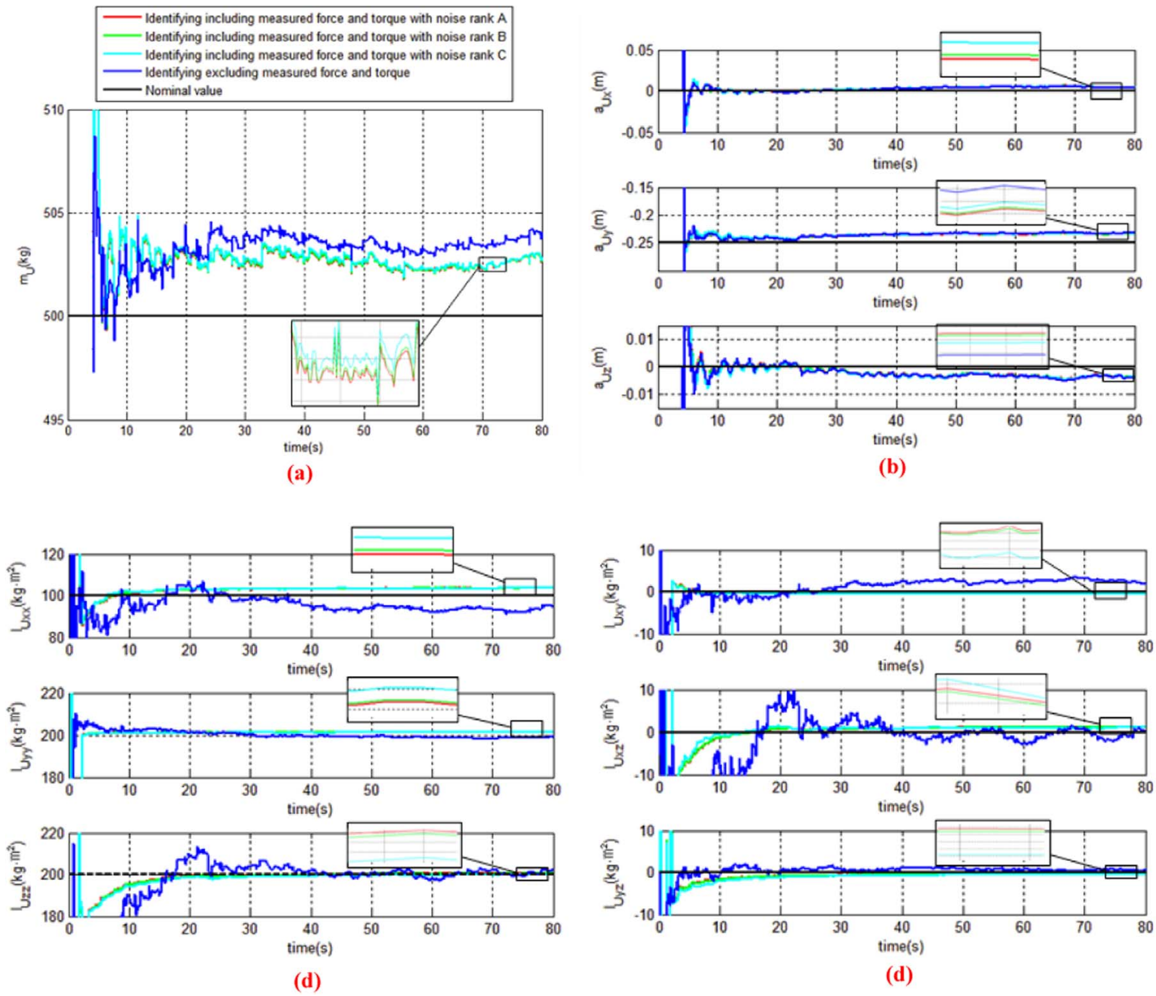

Fig. 8. Comparisons of modified identification via various ranks of measured noises of the force and torque.

estimation. The conventional identification scheme that only employs measured information of the spacecraft and manipulator will exhibit poor identification performance due to accumulated kinematic measurement errors and inertial estimation errors, as shown in the analysis of errors in this paper. Based on the MC method and momentum theorem in the post-capture phase, the contact force reacting on the surface of the unknown object together with the force/torque of the end-effector is used by modifying the conventional identification equation, reducing the accumulation of kinematic measurement errors and inertial estimation errors, and thereby improving the precision of the parameter identification. To ensure the stability of the identification process, a hybrid RLS-APSA algorithm is proposed and employed to decode the modified identification equation, considering various measured noises. Numerical simulation results verify the validity of the proposed method, effectively guaranteeing the execution of aerospace operations and preventing failed control, with the accuracy improvement achieved by introducing the contact force together with the force/torque of the end-effector and improving stability by employing the RLS-APSA algorithm.

Acknowledgment

This work was supported by the National Natural Science Foundation of China (NSFC) 51375034, 61327809., Innovation Foundation of Shanghai Aerospace Science Technology (SAST 2015-075)

References

[1] A. Flores-Abad, O. Ma, K. Pham, S. Ulrich, A review of space robotics technologies for on-orbit servicing, Prog. Aerosp. Sci. 68 (2014) 1–26.
[2] S. Dubowsky, E. Papadopoulos, The kinematics dynamics, and control of free-flying and free-floating space robotic systems, IEEE Trans. Robot. Autom. 9 (5) (1993) 531–543.
[3] L. Felicetti, P. Gasbarri, A. Pisculli, M. Sabatini, G.B. Palmerini, Design of robotic manipulators for orbit removal of spent launchers' stages, Acta Astronaut. 119 (2016) 118–130.
[4] C. Schedlinski, M. Link, A survey of current inertia parameter identification methods, Mech. Syst. Signal Process. 15 (1) (2001) 189–211.
[5] Y. Yu, T. Arima, S. Tsujio, Inertia parameters estimation of planar object on robot pushing operation, Int. J. Inf. Acquis. 6 (4) (2009) 239–247.
[6] Y. Murotsu, K. Senda, M. Ozaki, Parameter identification of unknown object handled by free-flying space robot, J. Guid. Control Dyn. 17 (3) (1994) 488–494.
[7] K. Yoshida, S. Abiko, Inertia parameter identification for a free-flying space robot, In: Proceedings of the AIAA Guidance, Navigation, and Control Conference and Exhibit, Monterey, CA, 2002.
[8] R. Lampariello, G. Hirzinger, Modeling and experimental design for the on-orbit inertial parameter identification of free-flying space robots, in: Proceedings of IDETC/CIE, ASME 2005 International Design Engineering Technical Conferences, 2005.
[9] O. Ma, H. Dang, On-orbit identification of inertia properties of spacecraft using a robotic arm, J. Guid. Control Dyn. 31 (6) (2008) 1761–1771.
[10] T.C. Nguyen-Huynh, I. Sharf, Adaptive reactionless motion and parameter identification, J. Guidance Control Dyn. 36 (2) (2013) 404–414.
[11] P.F. Huang, M. Wang, Z.J. Meng, F. Zhang, Z.X. Liu, Attitude takeover control for post-capture of target spacecraft using space robot, Aerosp. Sci. Technol. 51 (2016) 171–180.
[12] F. Aghili, K. Parsa, Motion and parameter estimation of space objects using laser-vision data, J. Guid. Control Dyn. 32 (2) (2009) 537–549.
[13] B.E. Tweddle, A. Saenz-Otereo, J.J. Leonard, D.W. Miller, Factor graph modeling of rigid-body dynamics for localization, mapping, and parameter estimation of a spinning object in space, J. Field Robot. 32 (6) (2015) 897–933.

[14] F. Zhang, I. Sharf, A. Misra, P. Huang, On-line estimation of inertia parameters of space debris for its tether-assisted removal, Acta Astronaut. 107 (2015) 150–162.
[15] D.K. Wang, P.F. Huang, J. Cai, Z.J. Meng, Coordinated control of tethered space robot using mobile tether attachment point in approaching phase, Adv. Sp. Res. 54 (6) (2014) 1077–1091.
[16] J. Sun, Y. Ma, S.J. Zhang, Z. Chu, Adaline network based identification method of inertial parameters for space uncooperative targets, Acta Aeronaut. Astronaut. Sin. (2016). http://dx.doi.org/10.7527/S1000-6893.2015.0349.
[17] P.S. Girao, P.M. Pinto Ramos, O. Postolache, J.M. Dias Pereira, Tactile sensors for robotic applications, Measurement 46 (2013) 1257–1271.
[18] G. Hirzinger, B. Brunner, J. Dietrich, Sensor-based space robotics-ROTEX and its telerobotics features, IEEE Trans. Robot. Autom. 9 (5) (1993) 649–662.
[19] H. Nakamoto, F. Kobayashi, N. Imamura, H. Shirasawa, F. Kojima, Universal robot hand equipped with tactile and joint torque sensors: development and experiment on stiffness control and object recognition, J. Syst. Cybern. Inform. 5 (2) (2007) 79–84.
[20] Y. Jung, D.G. Lee, J. Park, H. Ko, H. Lim, Piezoresistive tactile sensor discriminating multidirectional forces, Sensors 15 (2015) 25463–25473.
[21] D. Goeger, N. Ecker, H. Woern, Tactile sensor and algorithm to detect slip in robot grasping processes, in: Proceedings of the 2008 IEEE, International Conference on Robotics and Biomimetics, 2009, pp. 1480–1485.
[22] H. Huang, P. Fränti, D. Huang, S. Rahardja, Cascaded RLS–LMS prediction in MPEG-4 lossless audio coding, IEEE Trans. Audio Speech Lang. Process. 16 (3) (2008) 554–562.
[23] G. Ysebaert, K. Vanbleu, G. Cuypers, M. Moonen, T. Pollet, Combined RLS-LMS initialization for per tone equalizers in DMT-receivers, IEEE Trans. Signal Process. 51 (7) (2003) 1916–1926.
[24] S.H.K. Vemuri, I. Panahi, Hybrid RLS-NLMS algorithm for real-time remote active noise control using directional UltraSonic LoudSpeaker, in: Proceedings of the IECON 2014-40th Annual Conference of the IEEE, Industrial Electronics Society, 2014, pp. 2418–2424.
[25] E. Eweda, O. Macchi, Convergence of the RLS and LMS adaptive filters, IEEE Trans. Circuits Syst. 34 (7) (1987) 799–803.
[26] T. Shao, Y.R. Zheng, J. Benesty, An affine projection sign algorithm robust against impulsive interferences, IEEE Signal Process. Lett. 17 (4) (2010) 327–330.